School on Medical Physics for Radiation Therapy: Dosimetry, Treatment Planning and Delivery for Advanced Applications

ICTP

11 - 22 September 2023
An ICTP Meeting
Trieste, Italy

Further information:
http://indico.ictp.it/event/10205/
smr3871@ictp.it

Artificial intelligence in Radiotherapy

Michele Avanzo

Centro di Riferimento Oncologico di Aviano IRCCS, Aviano (PN), Italy



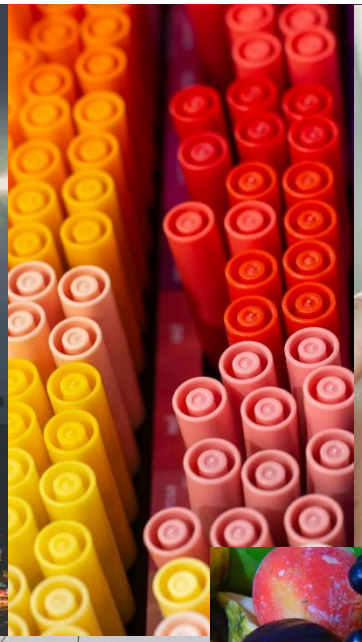



AI in Radiation Oncology

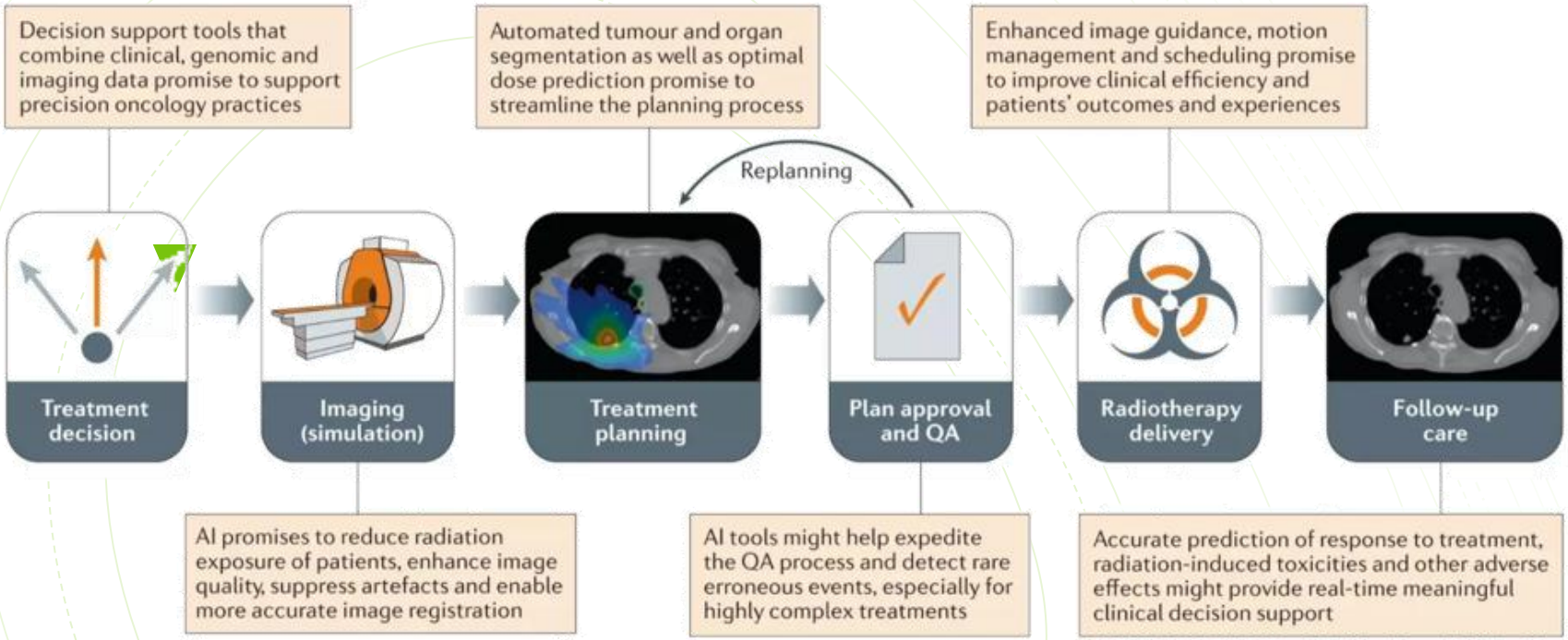

Huynh et al. Nat Rev Clin Oncol 2020

Treatment decision

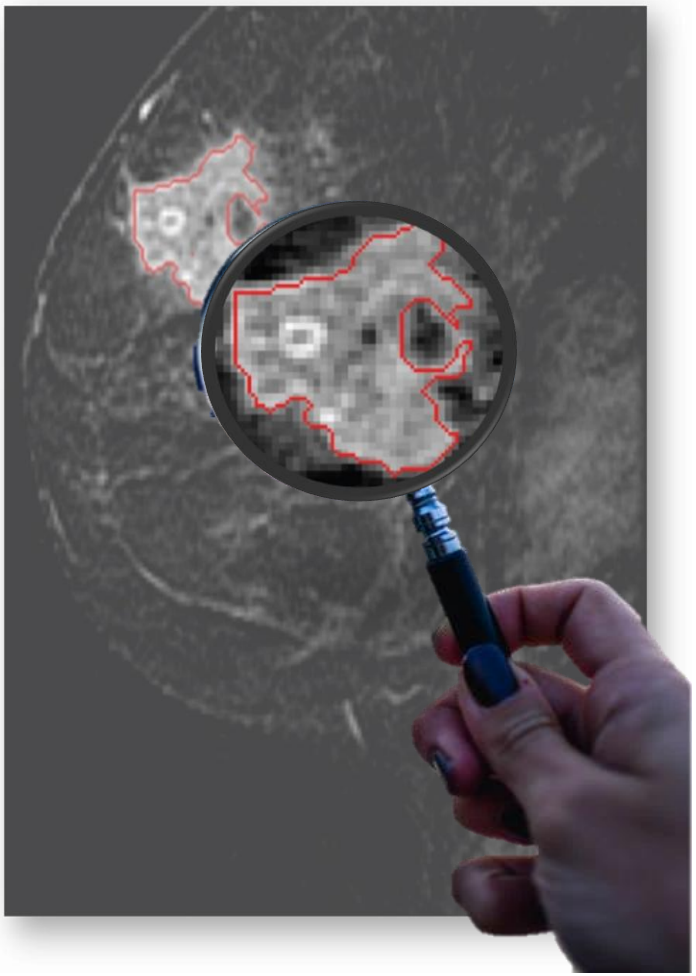

Treatment decision

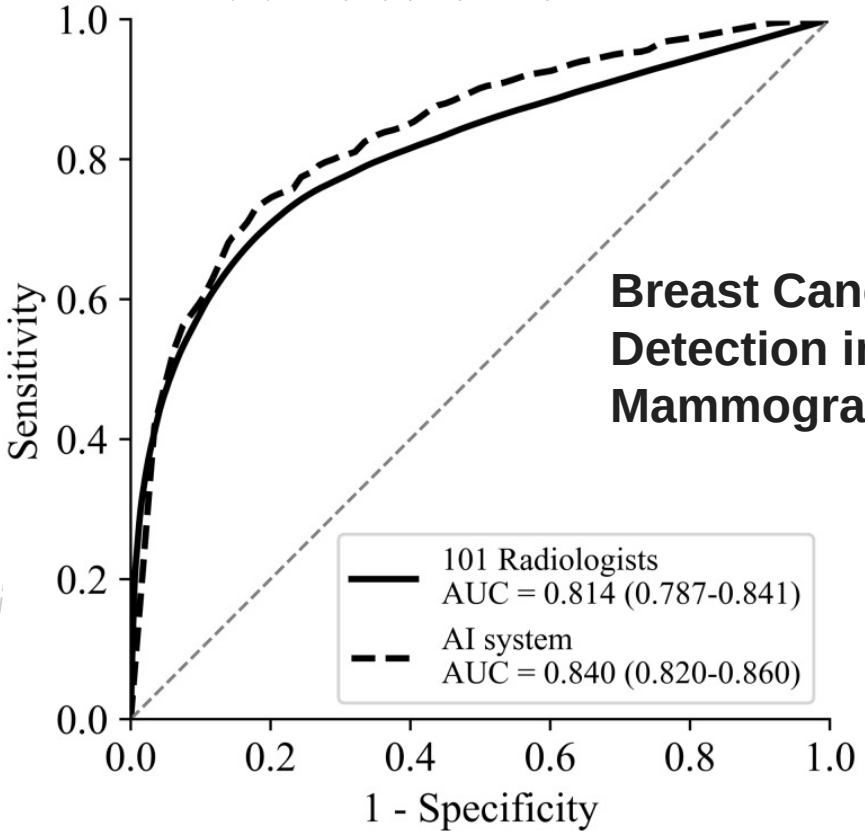

Figure 1. Receiver operating characteristic curve comparison between the reader-averaged radiologists and the artificial intelligence (AI) system in terms of area under the curve (AUC). Parentheses show the 95% confidence interval of the AUC.

Breast Cancer Detection in Mammography

ChatGPT in glioma adjuvant therapy decision making: ready to assume the role of a doctor in the tumour board?

Julien Haemmerli ,[1] Lukas Sveikata,[2,3,4] Aria Nouri,[1] Adrien May,[1] Kristof Egervari,[5] Christian Freyschlag,[6] Johannes A Lobrinus,[5] Denis Migliorini,[7] Shahan Momjian,[1] Nicolae Sanda,[2] Karl Schaller,[1] Sebastien Tran,[8] Jacky Yeung,[9] Philippe Bijlenga[1]

Rodriguez-Ruiz, JNCI J Natl Cancer Inst, 2019

Pre-Treatment imaging

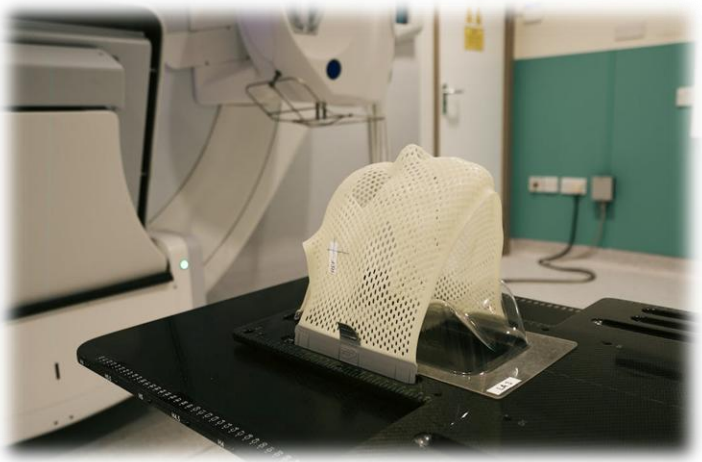

Conversion among imaging modalities

- GAN and autoencoders

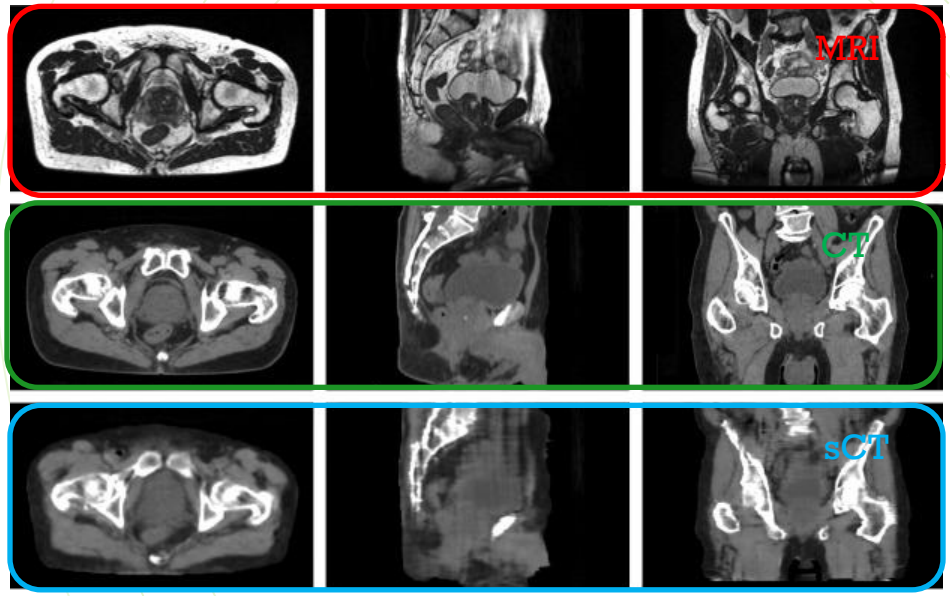

Cusumano et al. Radiotherapy and Oncology Volume 153, December 2020, Pages 205-212

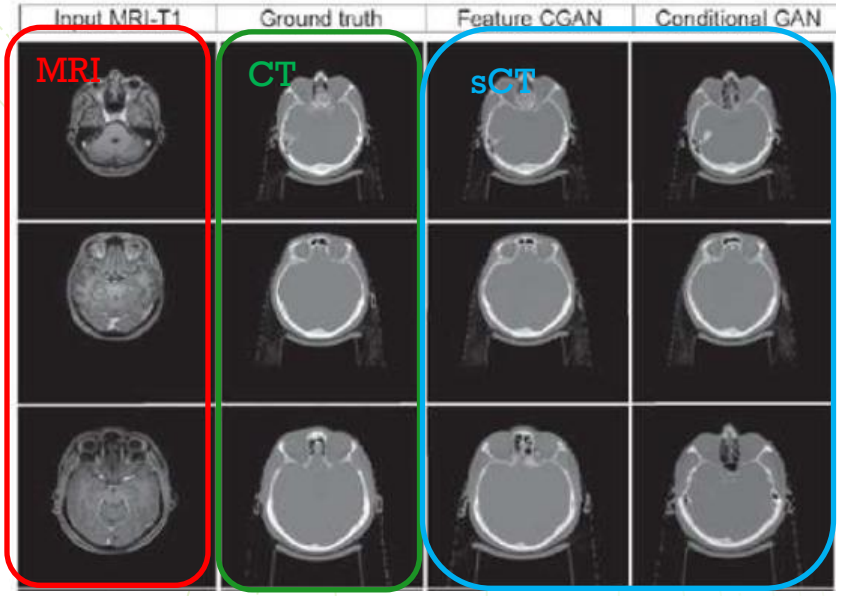

Fard et al., Computers in Biology and Medicine , Vol. 146, July 2022, 105556

Synthetic-CT generation for MR-only RT

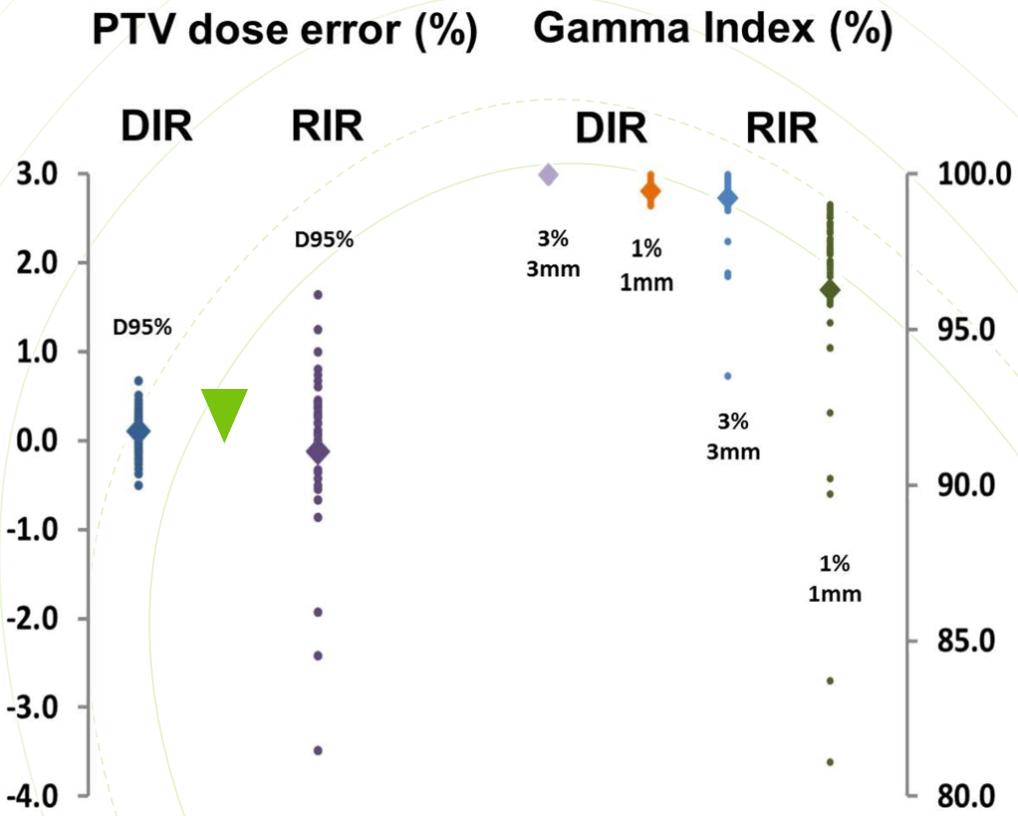

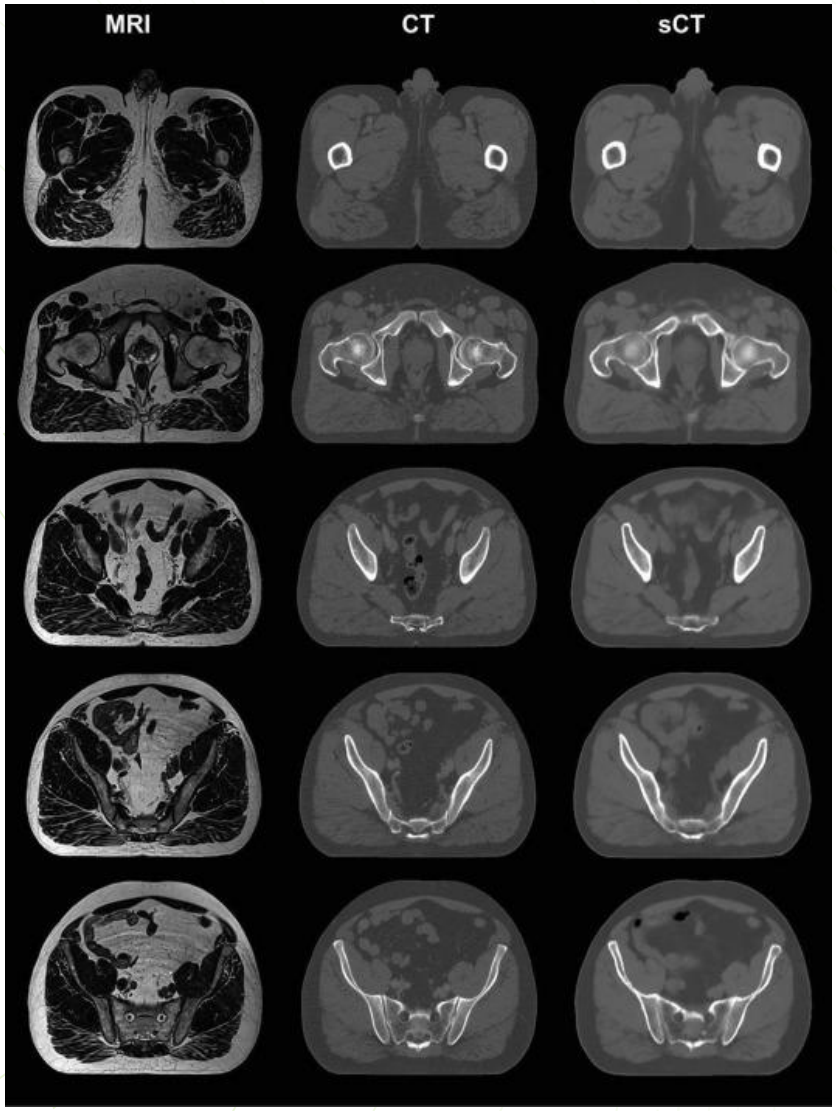

Bird, Radiotherapy and Oncology, 2021

Autocontouring: head and neck

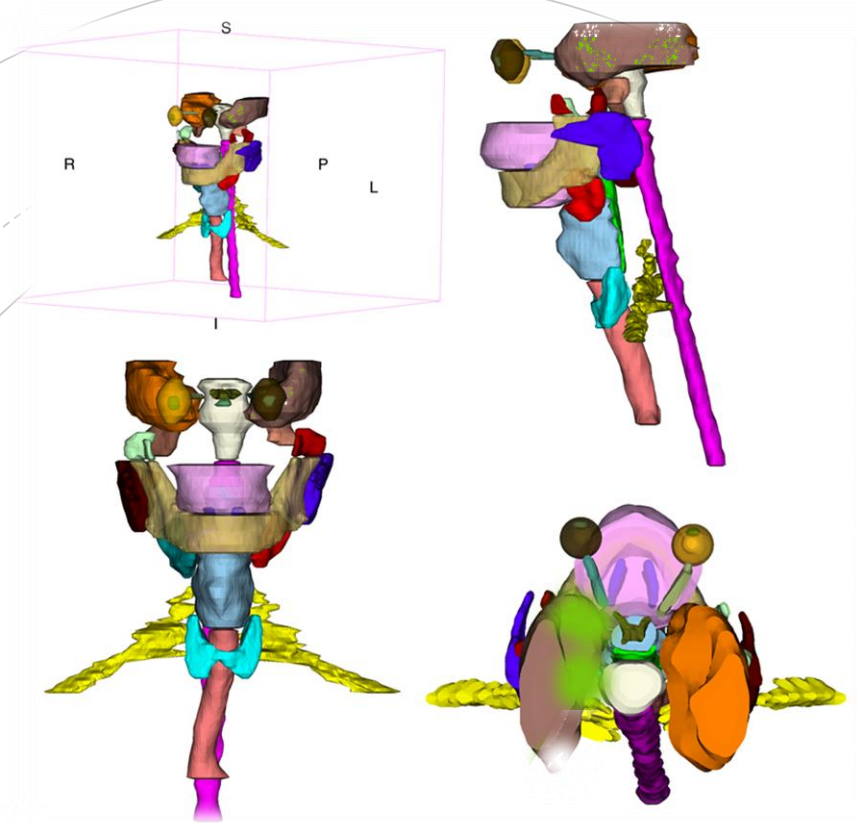

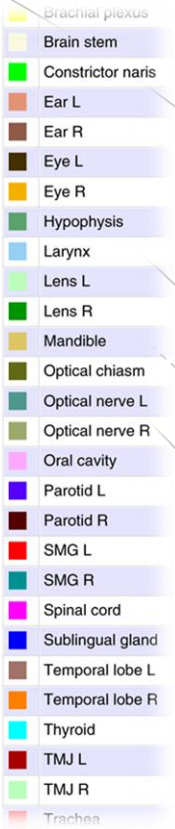

Tang, Nature Machine Intelligence 2019

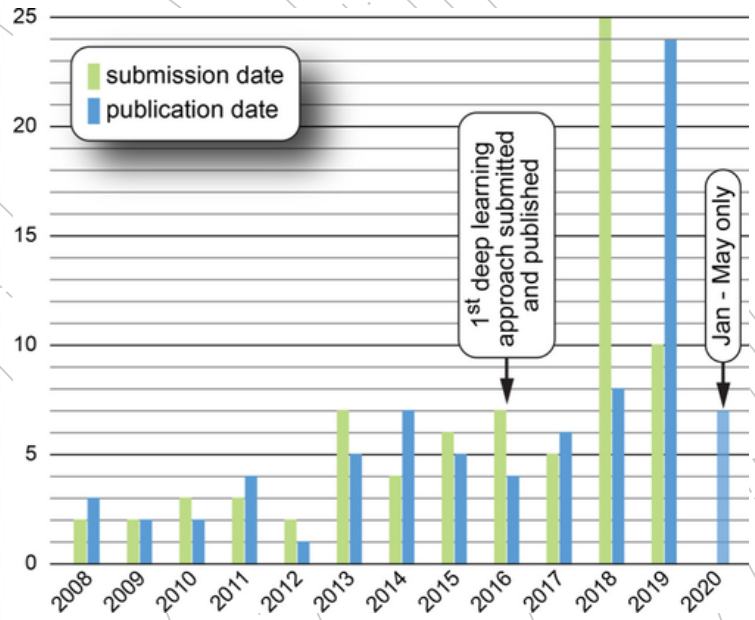

Vrtovec, Medical Physics 2020

Autocontouring: head and neck

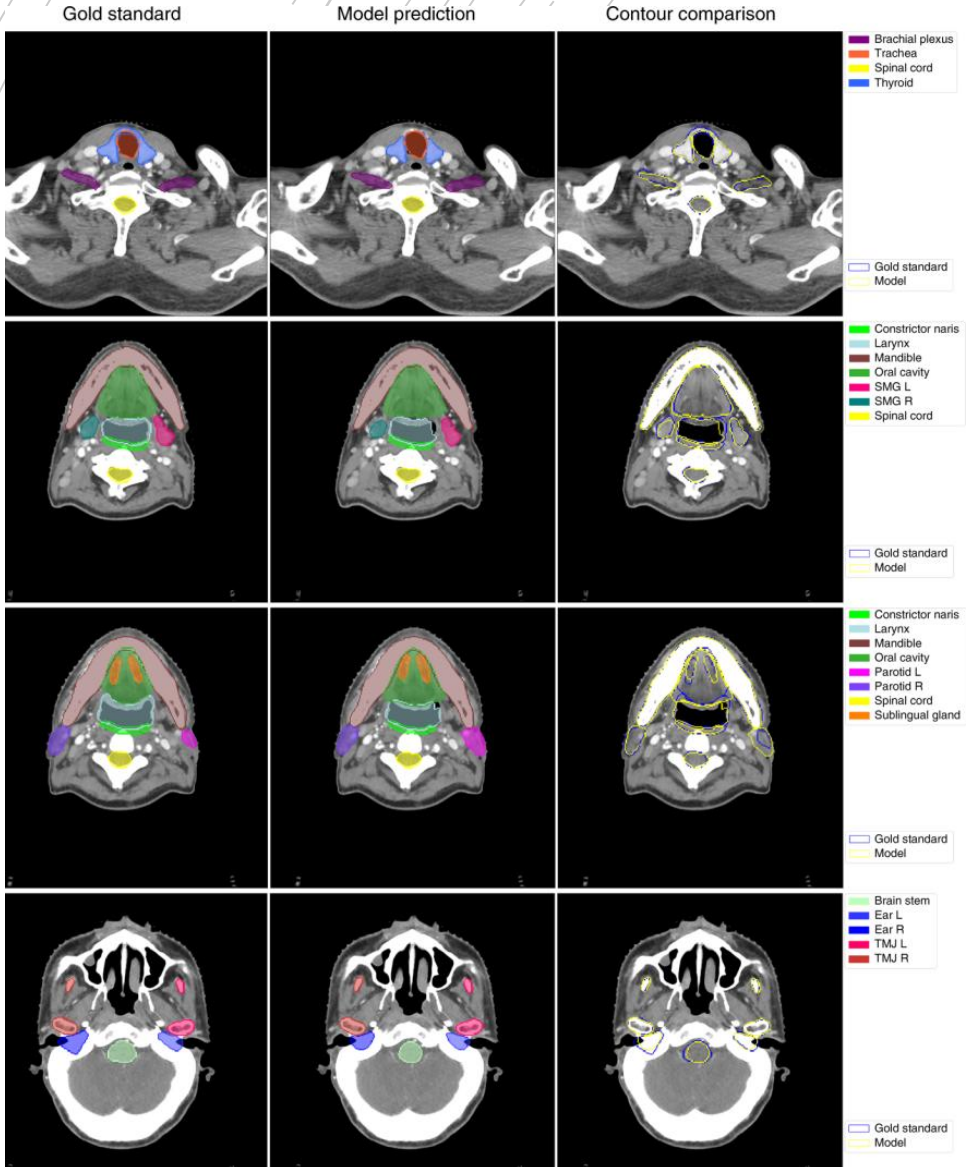

Table 3 | DSC comparison on the test set of dataset 1

OAR	MAS	AnatomyNet	U_a-Net	Human
Brachial plexus	30.38 ± 15.63	50.41 ± 8.08	**56.15 ± 10.83**	33.03 ± 7.83
Brain stem	82.25 ± 7.47	82.63 ± 4.57	**86.25 ± 3.86**	83.25 ± 4.63
Constrictor naris	66.38 ± 8.21	73.68 ± 7.56	**75.46 ± 6.13**	62.34 ± 8.63
Ear L	70.38 ± 14.94	76.68 ± 5.00	**77.28 ± 4.25**	43.57 ± 12.63
Ear R	70.03 ± 15.57	**78.77 ± 5.77**	78.64 ± 6.35	39.71 ± 10.81
Eye L	85.96 ± 10.99	88.41 ± 3.10	**92.51 ± 2.00**	90.71 ± 2.11
Eye R	82.68 ± 17.38	89.25 ± 3.38	**92.49 ± 2.34**	91.51 ± 1.79
Hypophysis	43.54 ± 18.45	56.18 ± 10.01	**63.86 ± 8.73**	59.26 ± 14.77
Larynx	82.60 ± 8.19	83.06 ± 7.98	**89.25 ± 3.26**	68.60 ± 6.59
Lens L	46.25 ± 24.29	77.25 ± 7.92	**81.90 ± 6.88**	64.27 ± 10.06
Lens R	45.53 ± 23.94	78.06 ± 7.51	**83.04 ± 5.90**	71.79 ± 9.59
Mandible	83.95 ± 11.48	91.97 ± 1.71	**93.12 ± 1.41**	90.97 ± 1.46
Optic chiasm	42.08 ± 17.52	60.55 ± 11.16	64.21 ± 16.39	28.61 ± 14.40
Optic nerve L	59.49 ± 14.61	72.55 ± 6.55	**75.73 ± 7.26**	65.10 ± 8.44
Optic nerve R	59.08 ± 16.53	72.95 ± 7.90	**76.06 ± 6.49**	66.14 ± 7.29
Oral cavity	86.10 ± 9.11	87.69 ± 5.67	**90.77 ± 2.32**	79.30 ± 3.59
Parotid L	72.52 ± 15.57	82.28 ± 6.71	**84.86 ± 4.22**	78.46 ± 4.90
Parotid R	71.20 ± 17.55	82.20 ± 7.26	**84.93 ± 3.99**	78.88 ± 4.41
SMG L	60.89 ± 12.11	75.47 ± 8.93	**80.71 ± 7.32**	77.73 ± 6.25
SMG R	63.70 ± 15.80	74.82 ± 14.69	**82.54 ± 7.47**	74.10 ± 16.92
Spinal cord	77.42 ± 16.70	80.32 ± 6.48	**85.64 ± 5.90**	84.59 ± 6.62
Sublingual gland	21.52 ± 16.34	39.94 ± 21.02	**45.99 ± 18.84**	35.16 ± 23.87
Temporal lobe L	80.05 ± 7.28	81.76 ± 5.33	**84.78 ± 2.62**	82.41 ± 5.01
Temporal lobe R	78.26 ± 7.40	72.97 ± 14.60	**84.13 ± 3.34**	80.90 ± 7.49
Thyroid	63.68 ± 19.65	71.82 ± 11.40	**85.62 ± 4.63**	82.42 ± 6.16
TMJ L	61.26 ± 19.86	86.65 ± 3.34	**87.96 ± 3.12**	84.67 ± 5.09
TMJ R	63.45 ± 20.48	85.73 ± 3.69	**86.86 ± 3.60**	81.98 ± 8.59
Trachea	65.86 ± 18.75	79.34 ± 7.75	81.29 ± 4.84	**91.05 ± 1.69**
Average	64.87	76.19	80.43	70.38

Values are given in units of %. L, left; R, right; SMG, submandibular gland; TMJ, temporomandibular joint; MAS, multi-atlas segmentation. Bold numbers represent oncologist modified his/her previous delineation by referencing the corresponding MRI images.

Tang, Nature Machine Intelligence 2

Autocontouring: bhead and neck

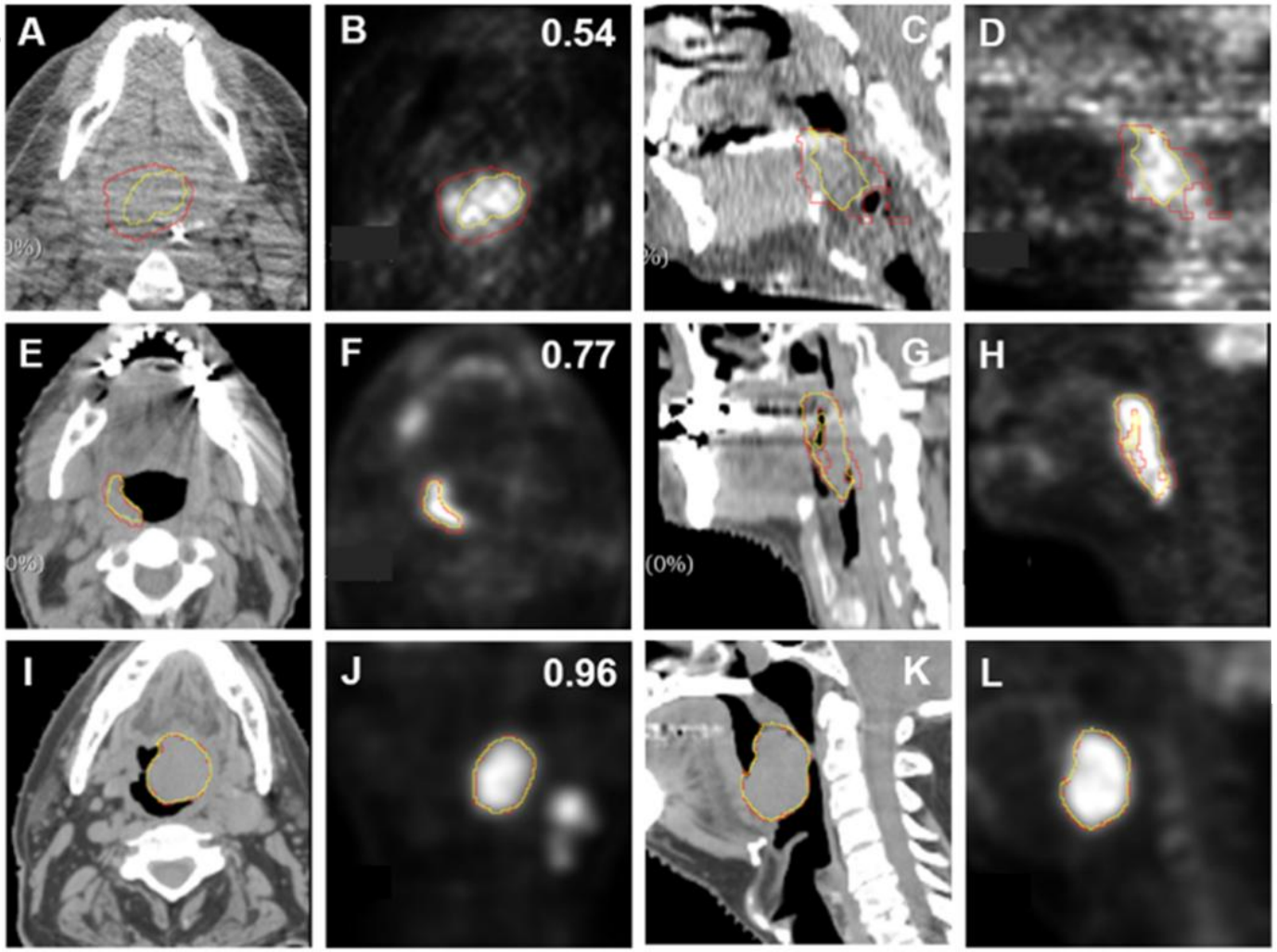

256 and 512 ResUnet mod

Model	DSC
256 (mean)	0.771 ± 0.039
256 (median)	0.829 ± 0.024
512 (mean)	0.768 ± 0.041
512 (median)	0.828 ± 0.024

Naser, Head Neck Tumor Segm Chall (2021)

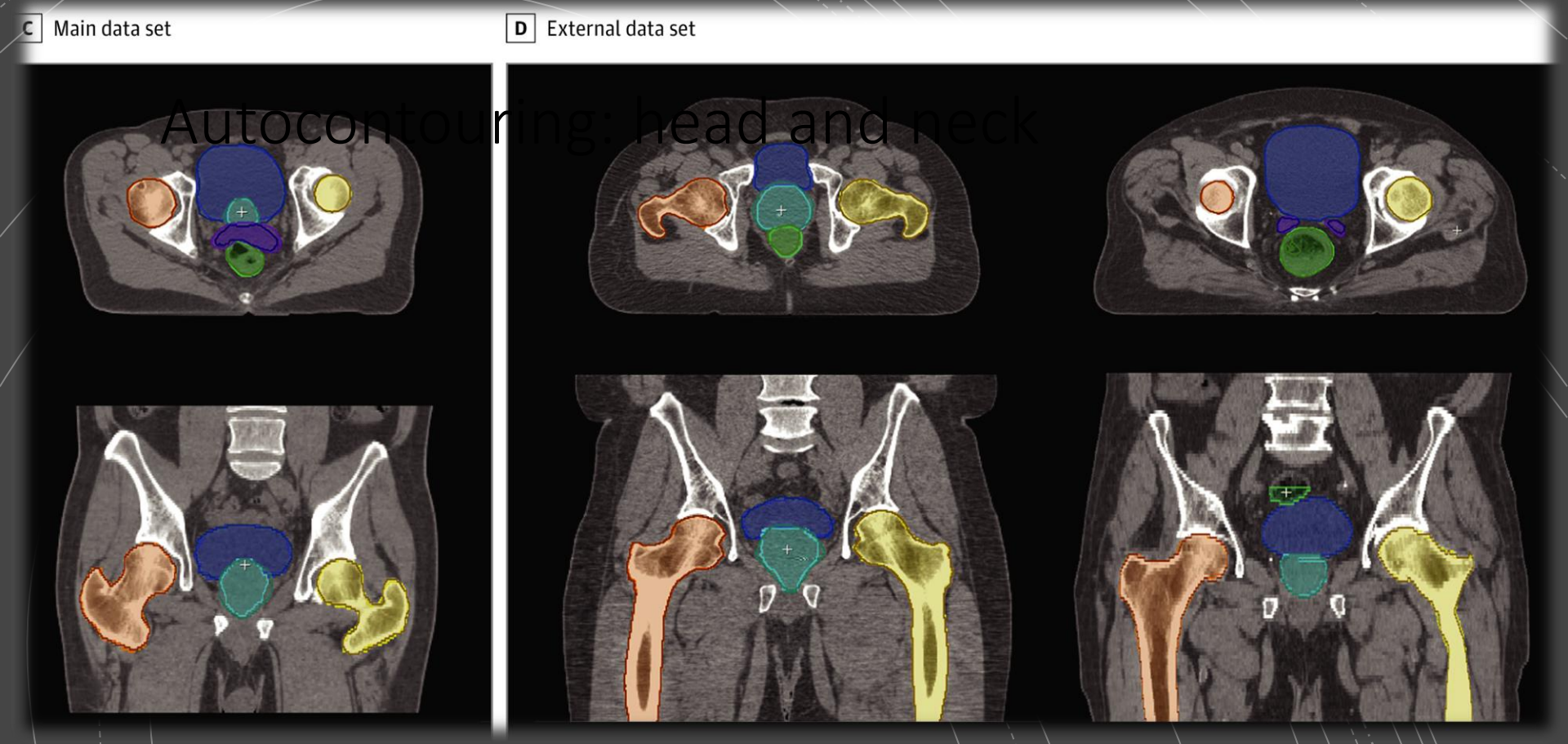

Autocontouring: head and neck

Autocontouring: pelvis

Oktay, JAMA Netw Open. 2020

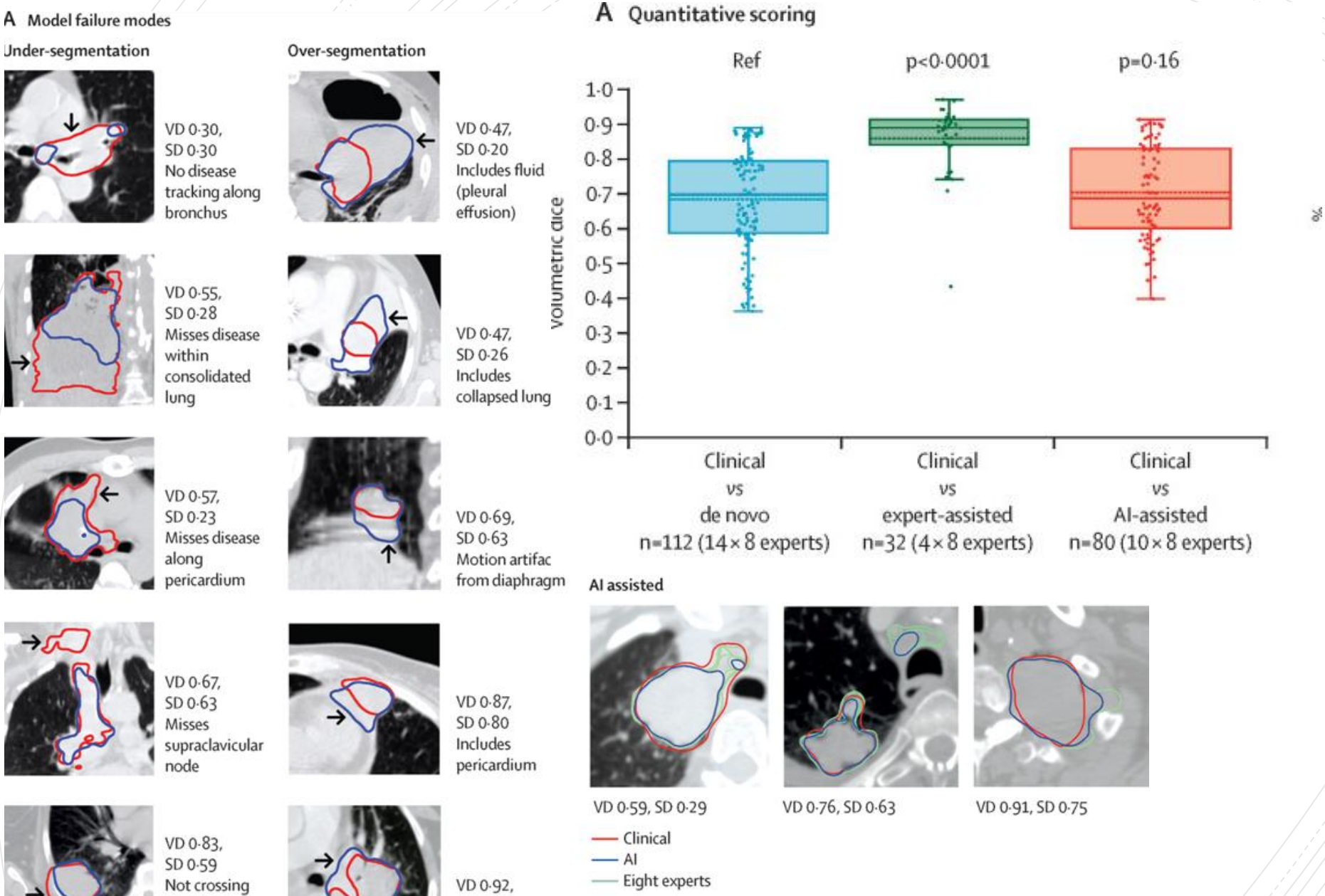

Autocontouring: failure modes

Hosny, Lancet Digit Health 2022

Autocontouring: brain

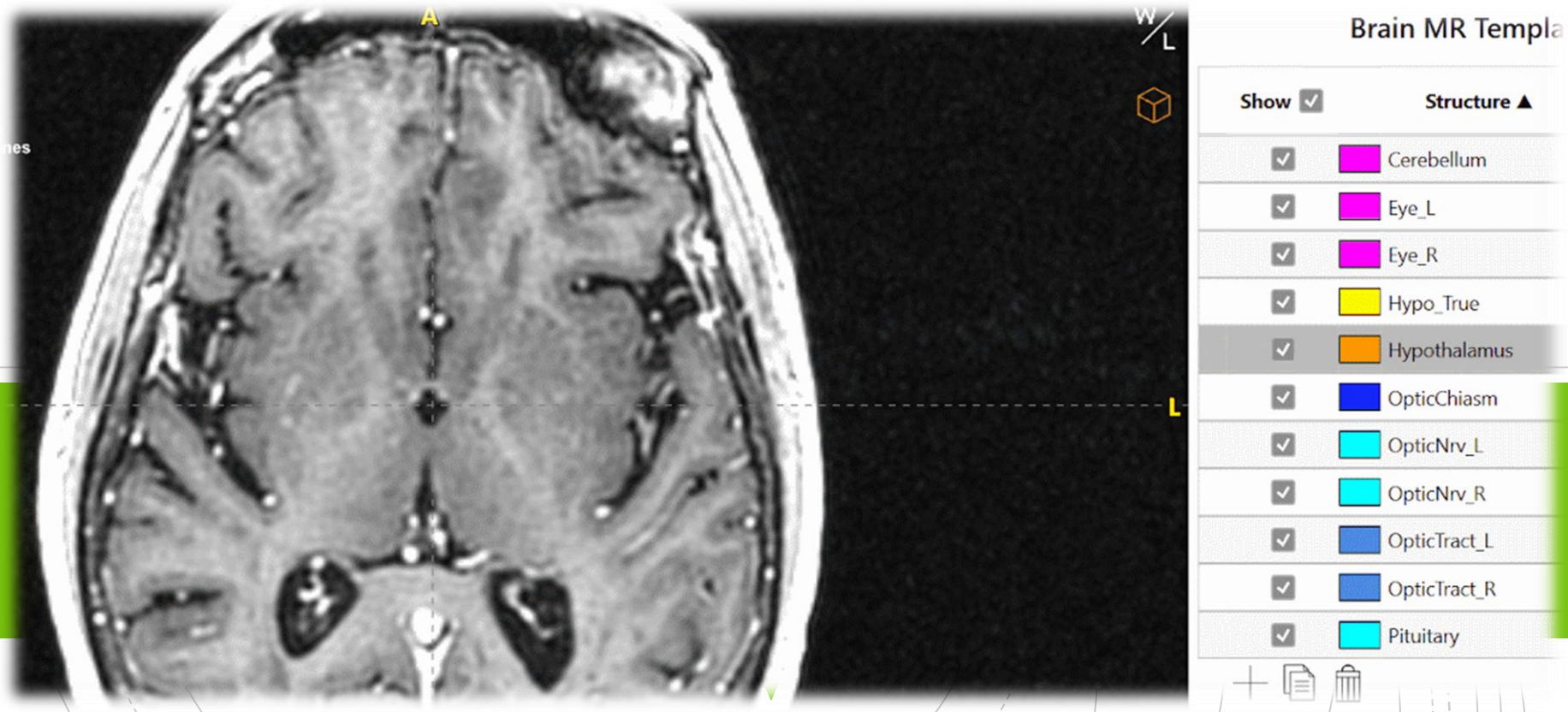

https://blog.radformation.com/autocontour-adds-to-the-list-of-available-structures

Autocontouring: abdomen

https://blog.radformation.com/autocontour-adds-to-the-list-of-available-structures

Autocontouring: MRI, DRR

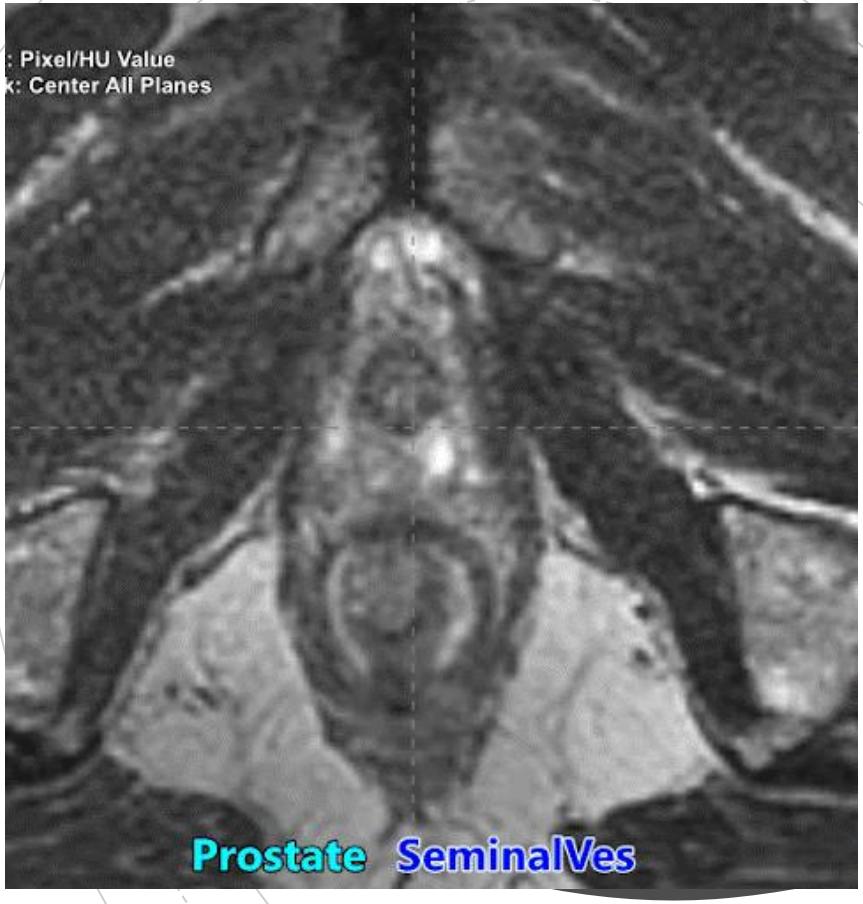

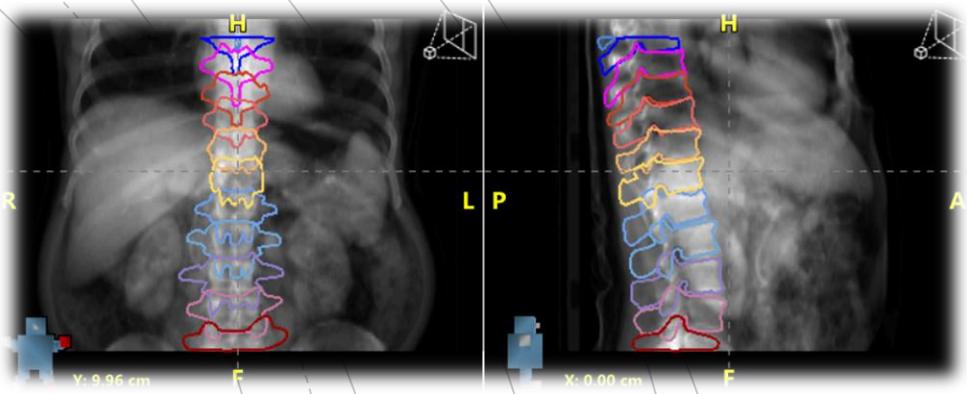

https://blog.radformation.com/autocontour-adds-to-the-list-of-available-structures

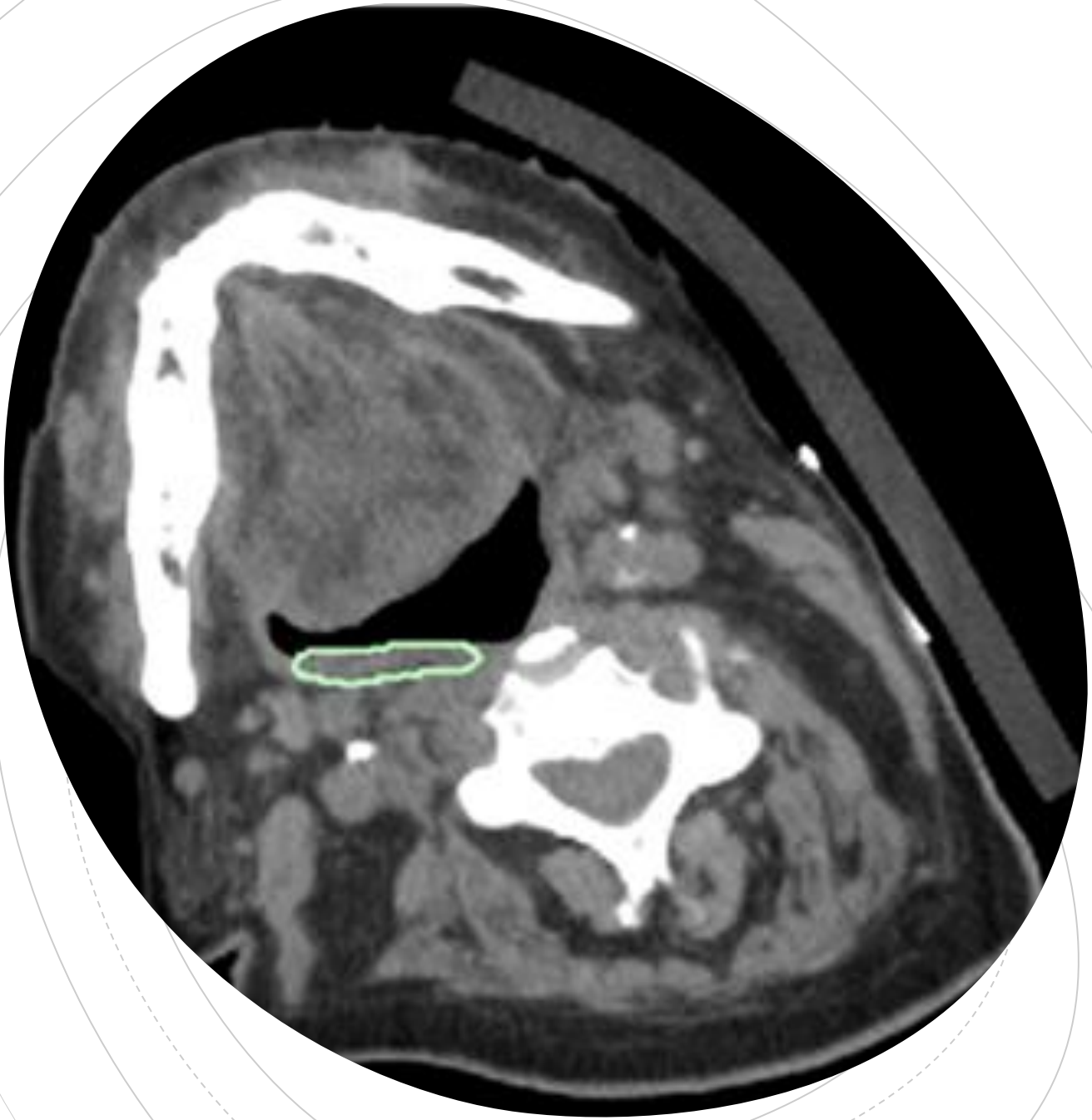

pharyngeal constrictor muscle in wrong place

Michael Gensheimer
@MFGensheimer

Patient selection for proton therapy

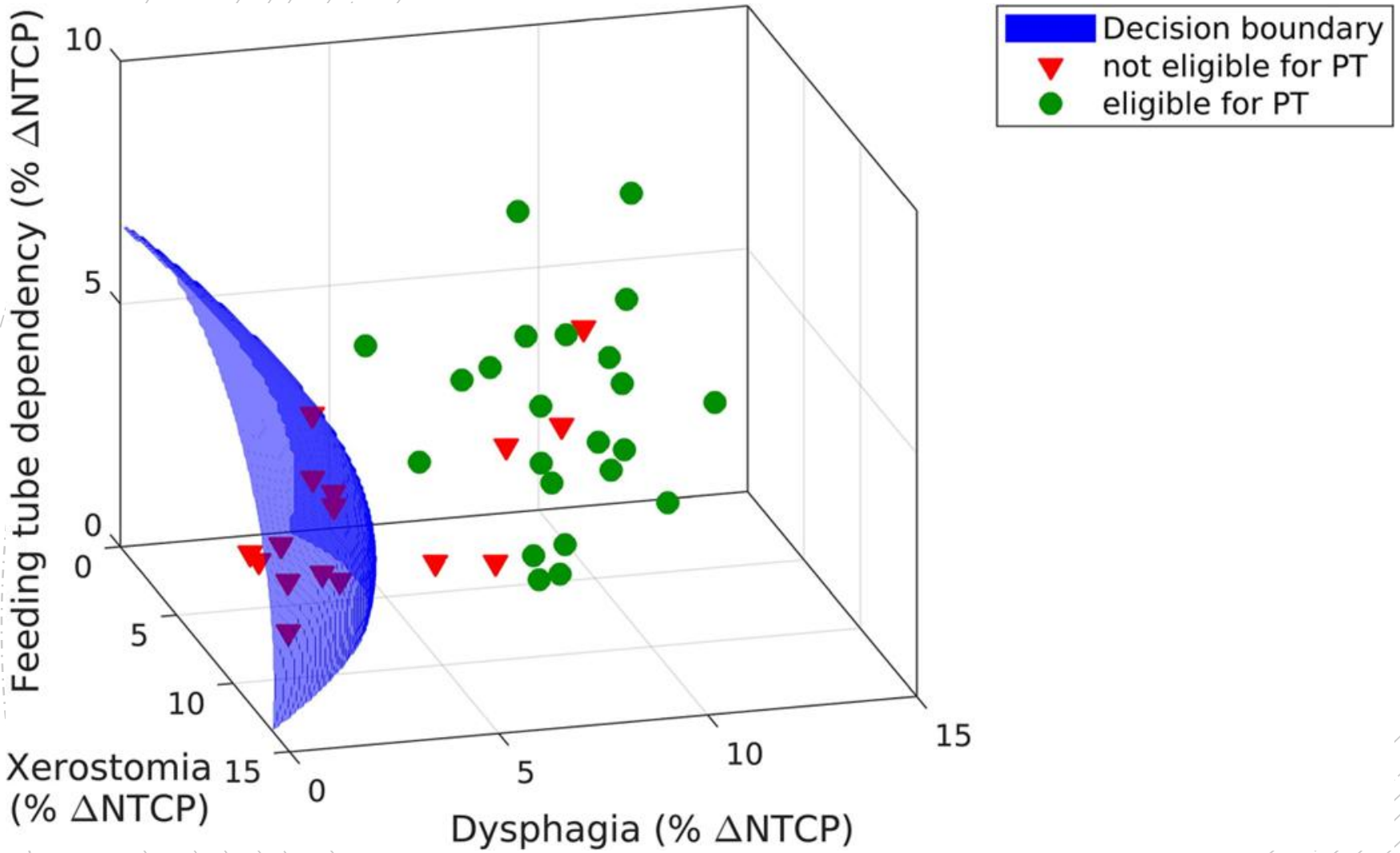

Kouwenberg, Radiotherapy and Oncology, 2021

Patient selection for proton therapy

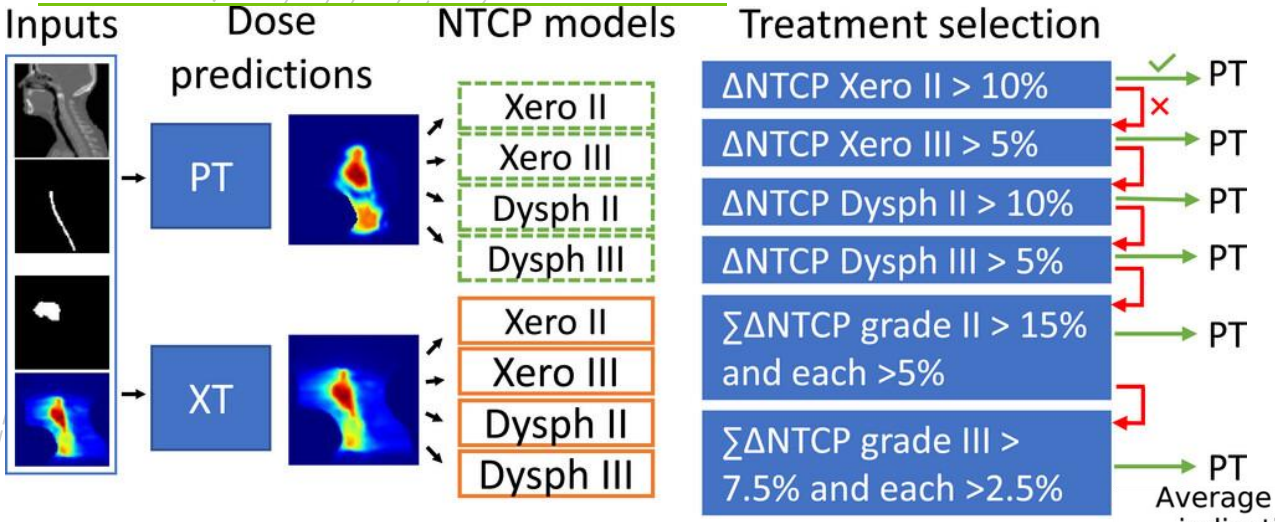

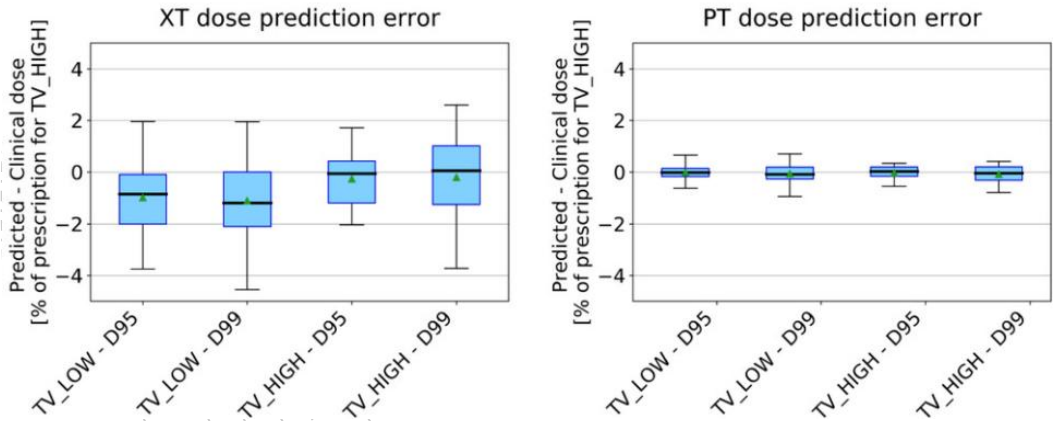

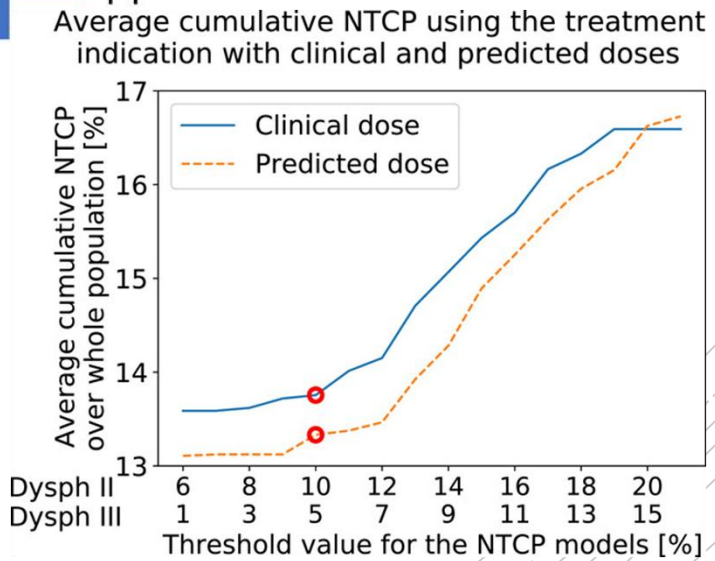

Huet-Dastarac, Medical Physics, 2021

Radiotherapy treatment planning

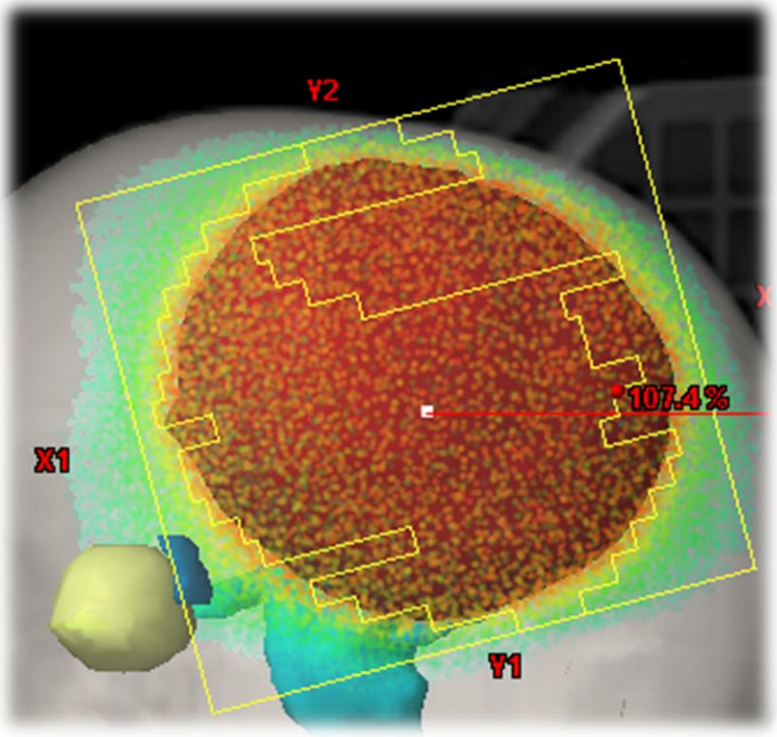

Dose prediction

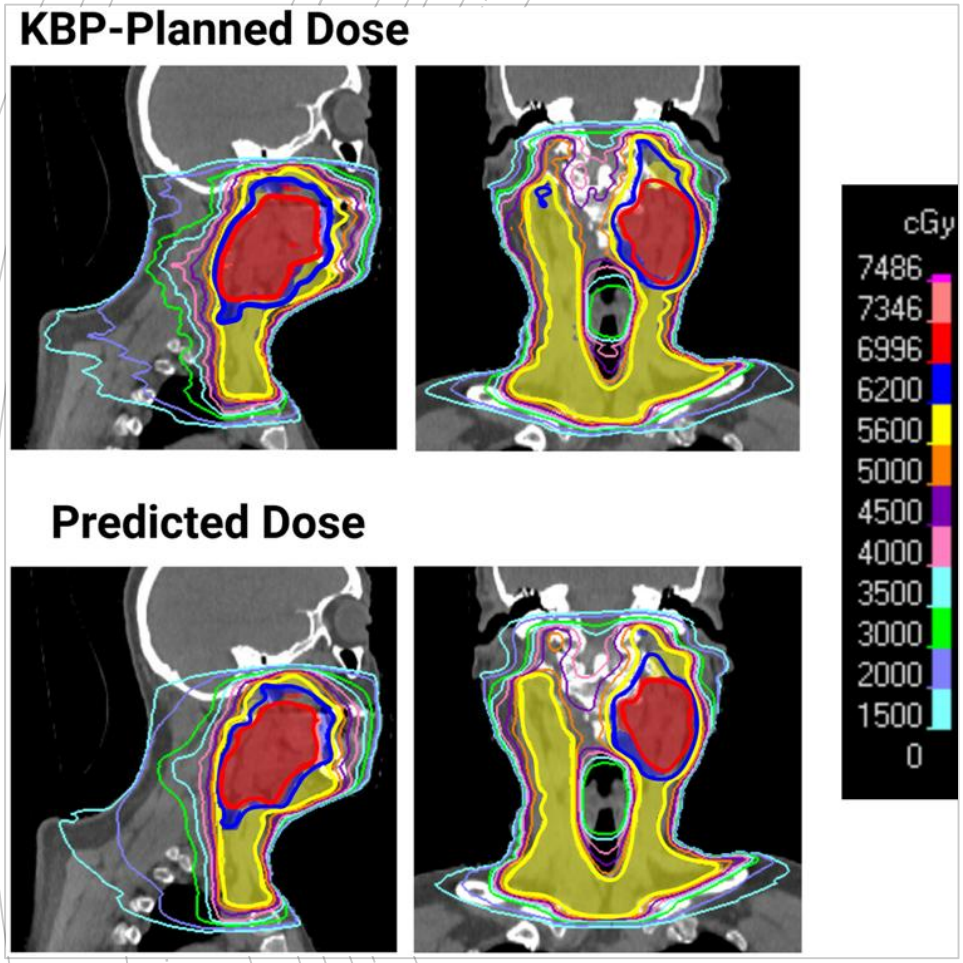

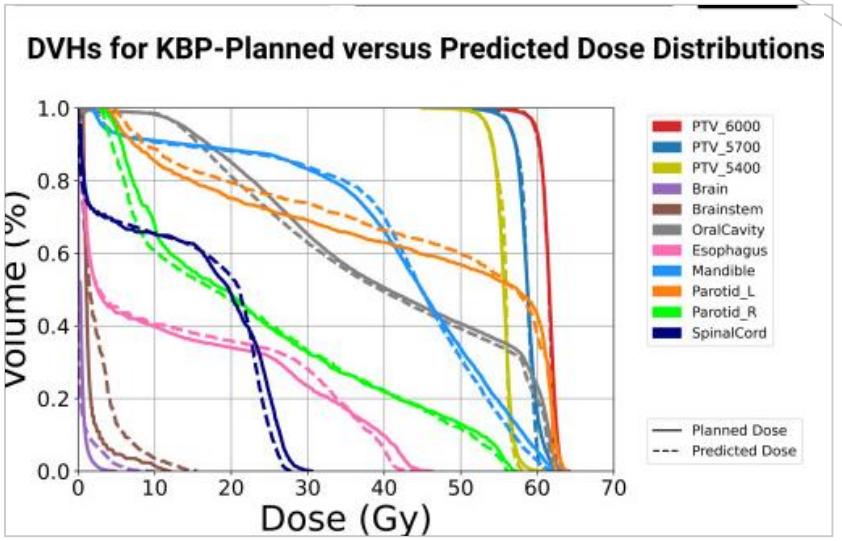

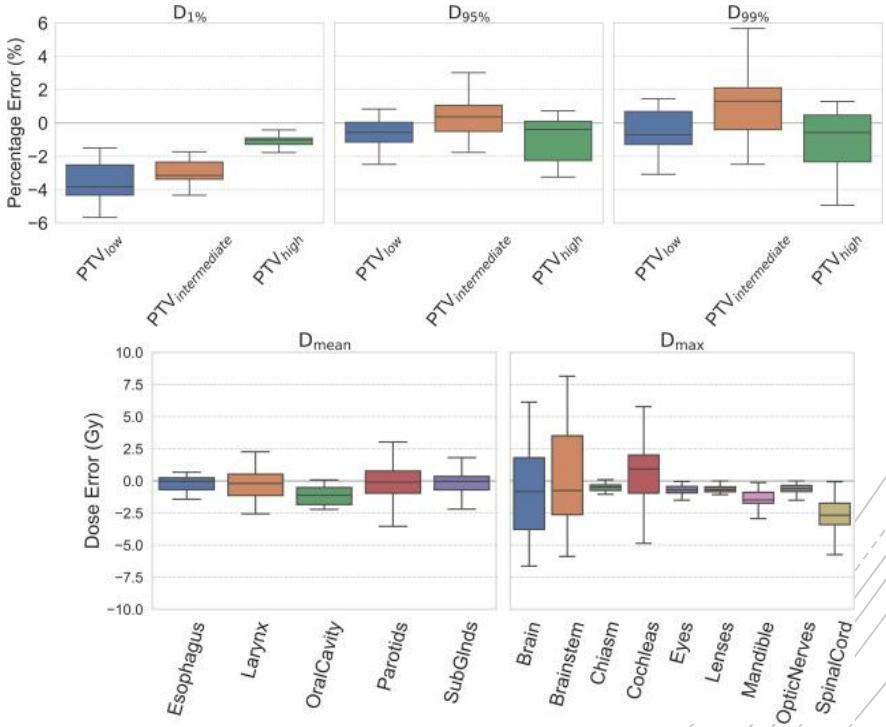

- Gronberg, Practical Rad.Onc. 2023

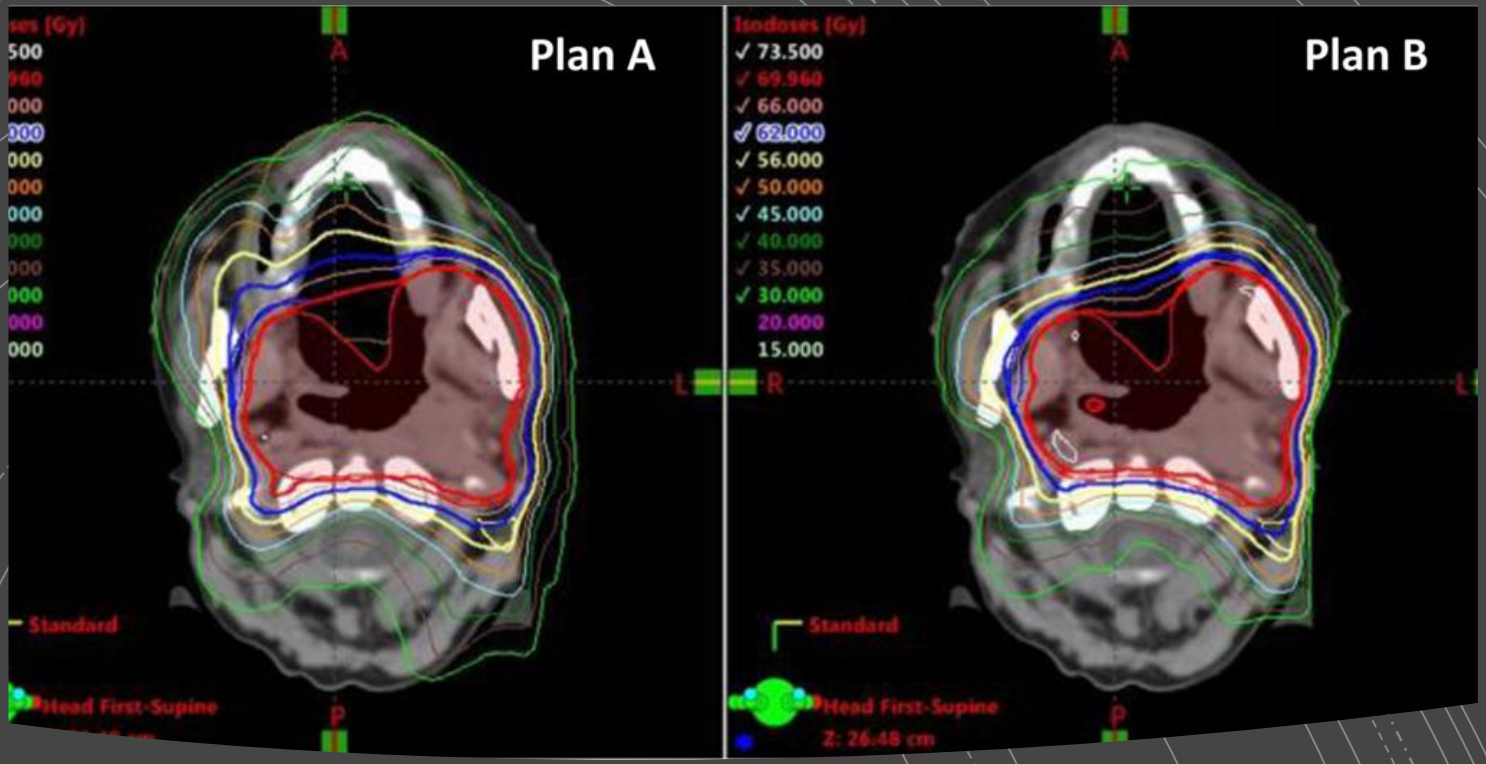

Automated planning

- Figure clinical plan vs autoplan. Both were judged to be acceptable plans, with preference for the autoplan based on reduced dose to the oral cavity and posterior neck.

Olanrewaju, Pract Radiat Oncol. 2021

Dose prediction/autoplanning

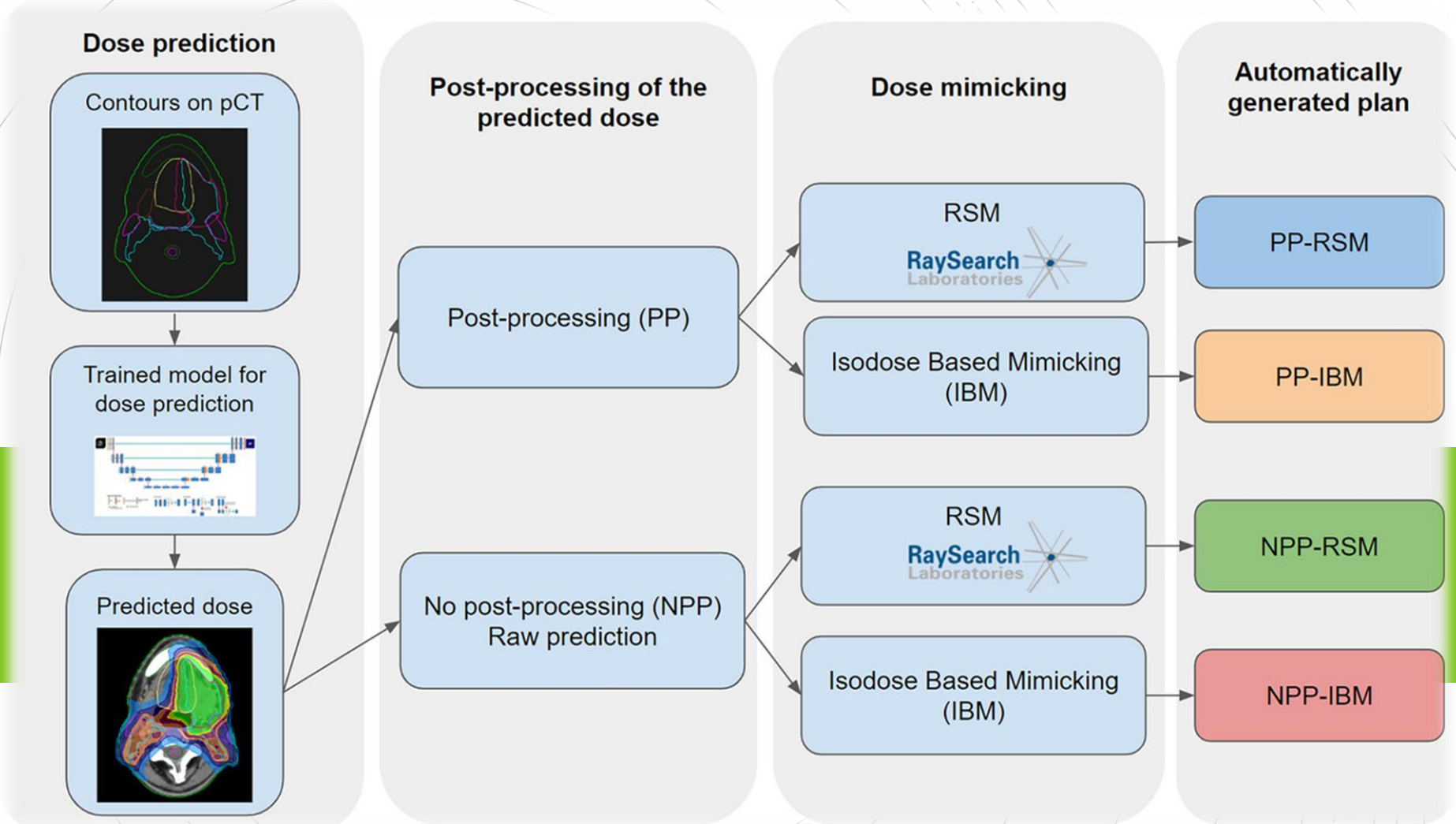

Borderias-Villarroel, Medical Physics 2023

Fully automated RT workflow

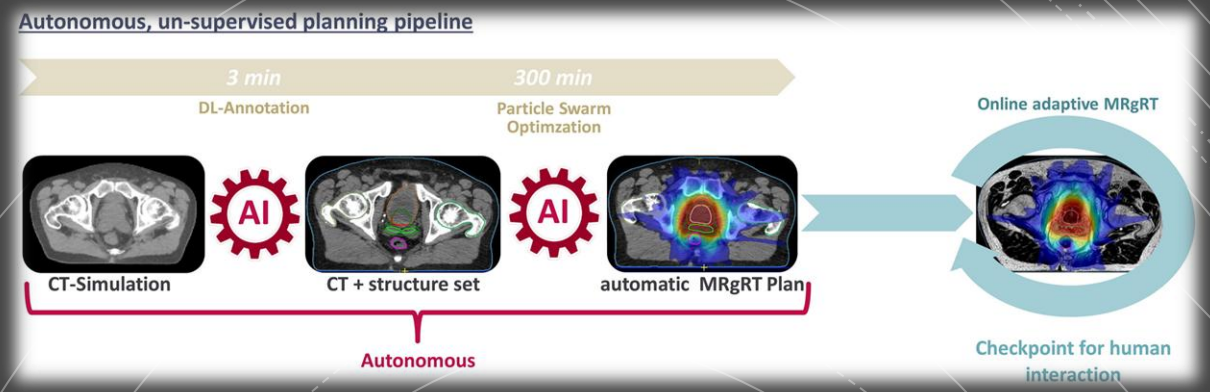

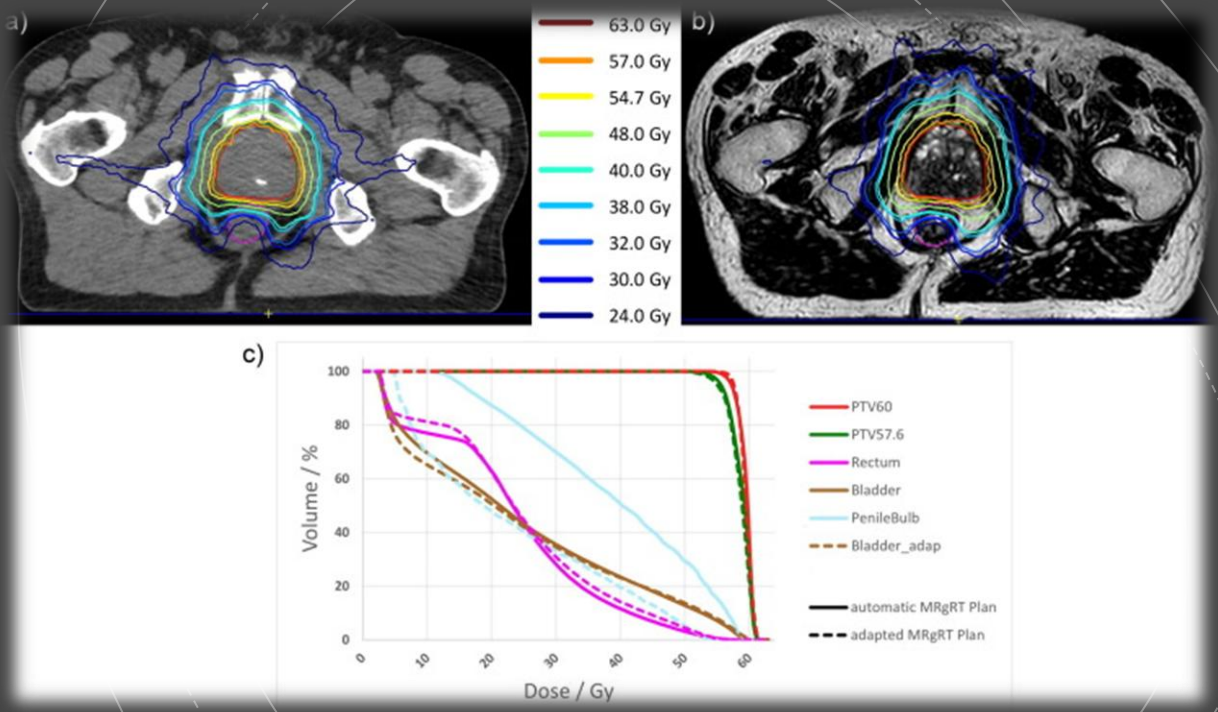

- Autonomous plan generation, including OAR segmentation, target generation and optimization
- First checkpoint for human interaction at the time of clinical online adaptation at the MR-Linac.

Kunzel, Radiotherapy and Oncology, 2021

Prediction of acute toxicity to the rectum

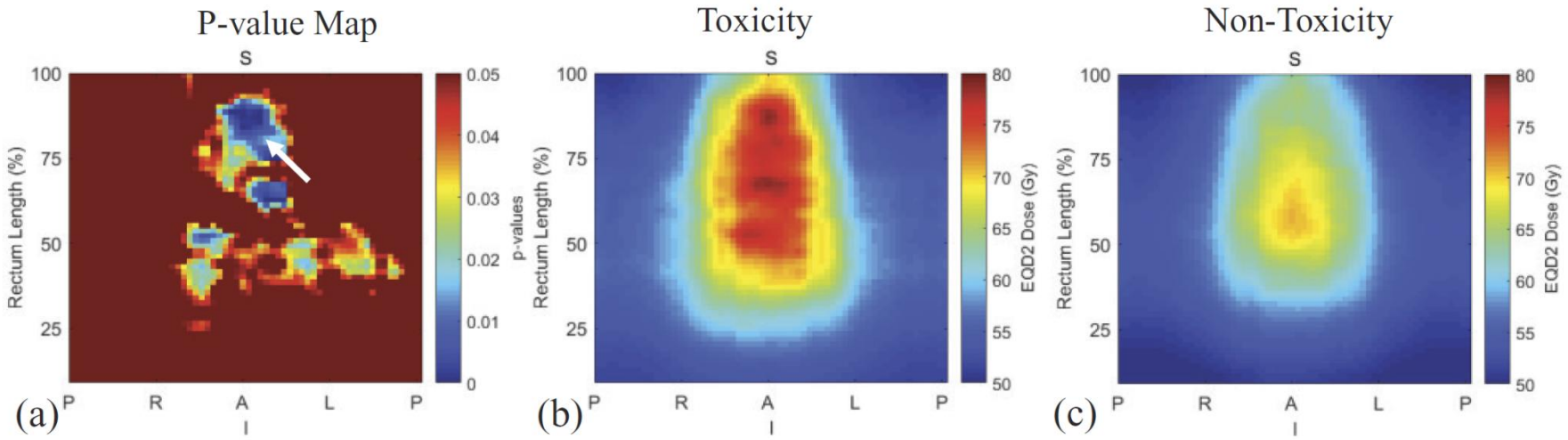

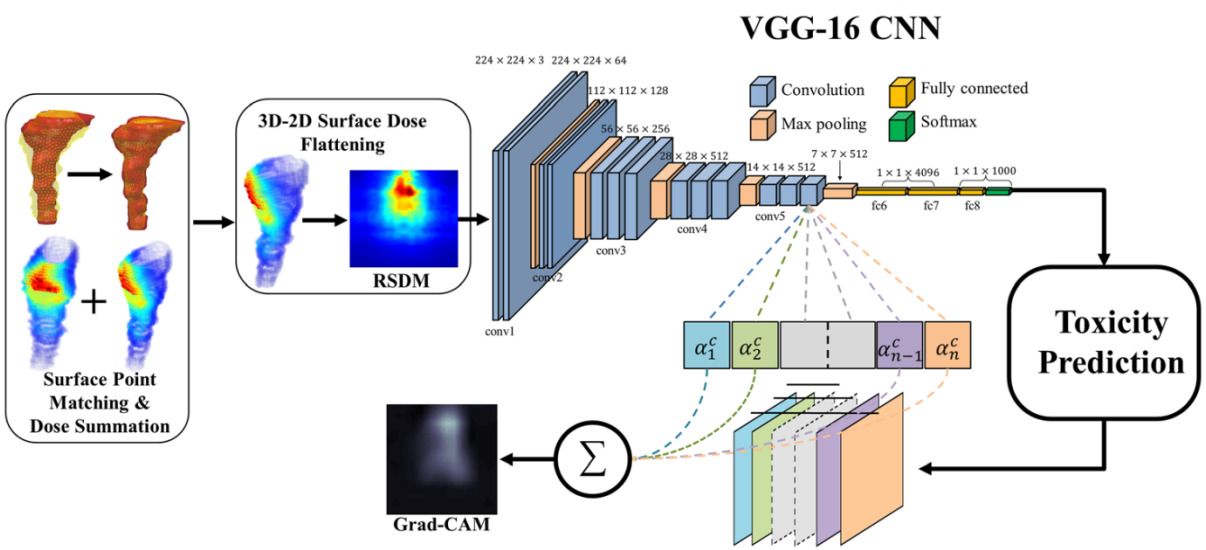

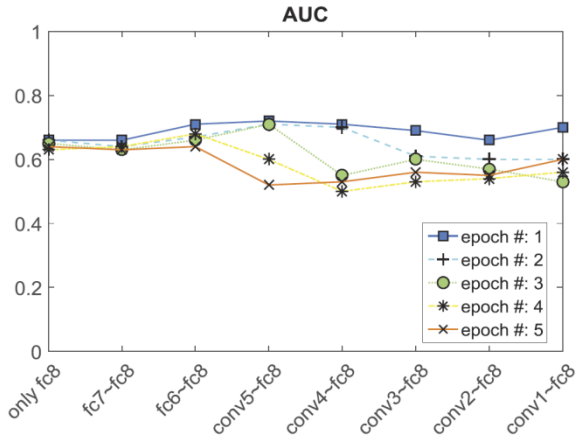

Zhen, Phys. Med. Biol. 62 (2017) 8246

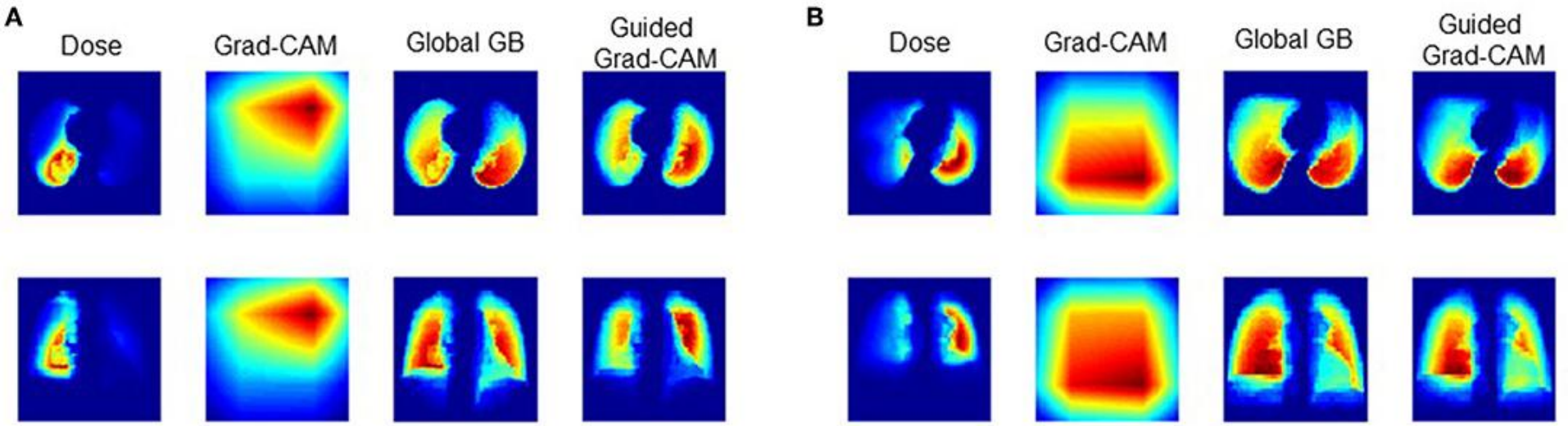

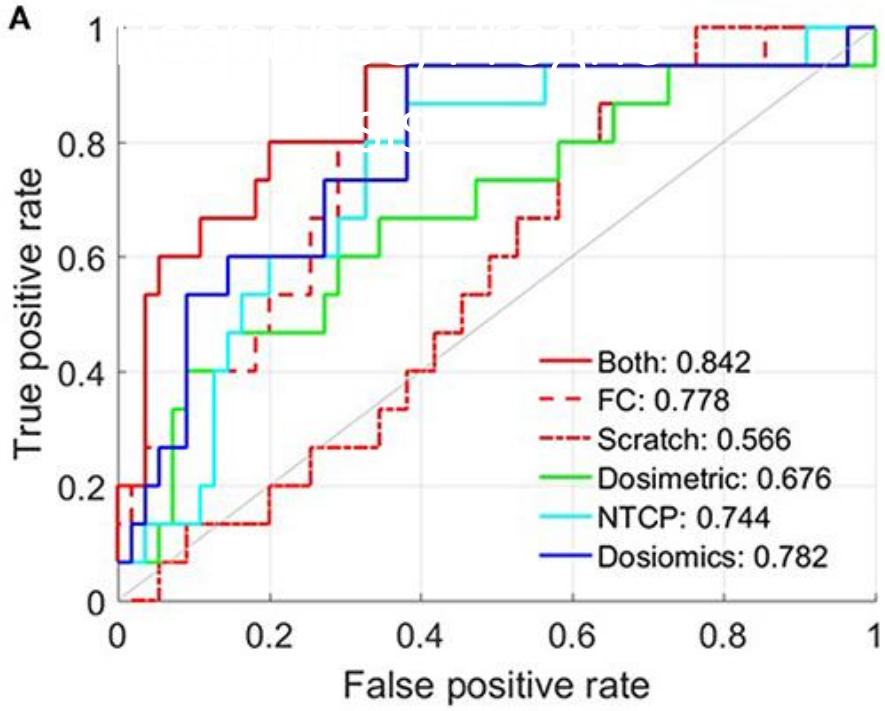

Prediction of
lung toxicity (fibrosis)

Liang, Front. Oncol., 2020

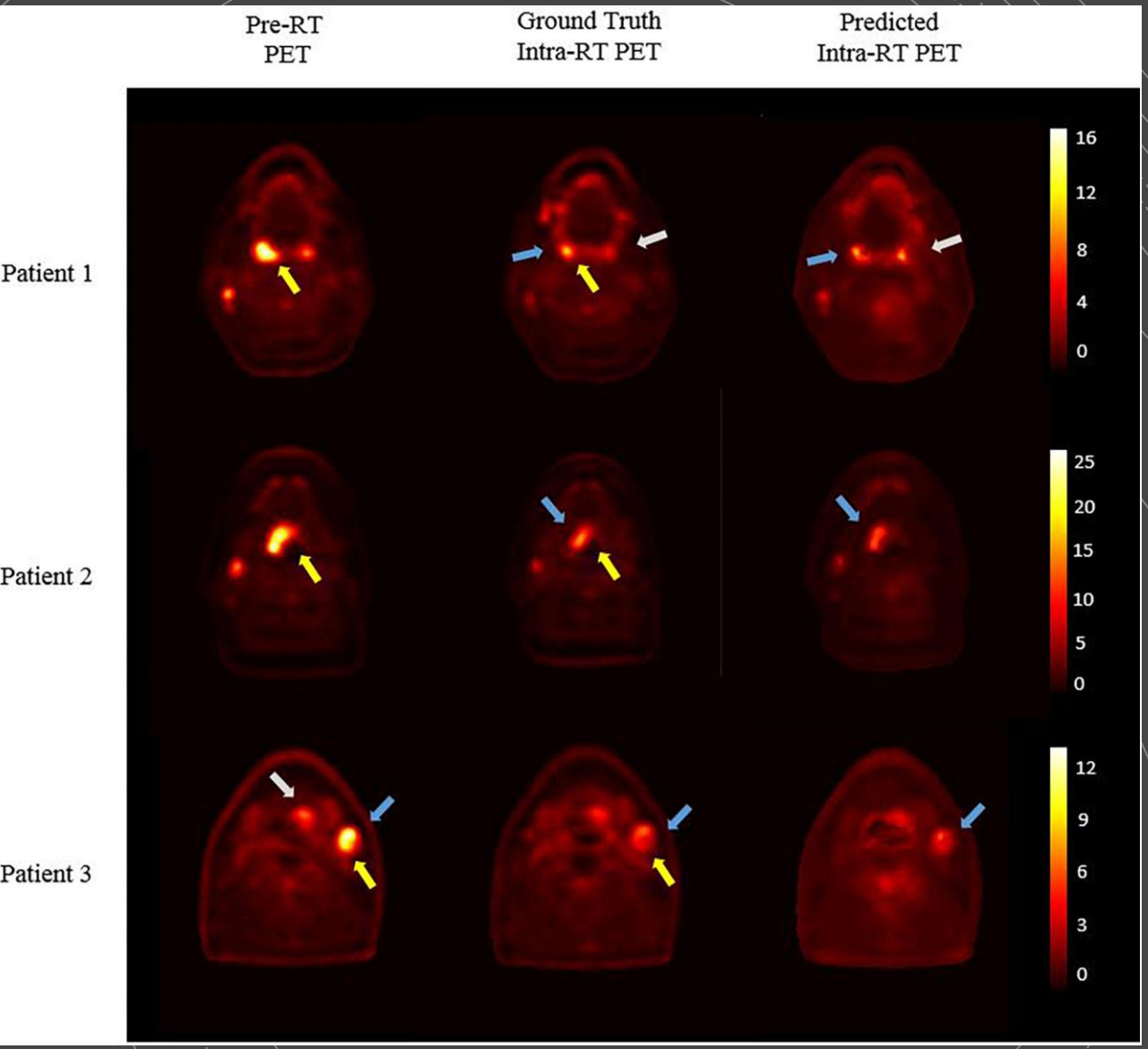

Prediction of tumor response in PET

Wang, Front. Oncol., 2020

Dose prescription

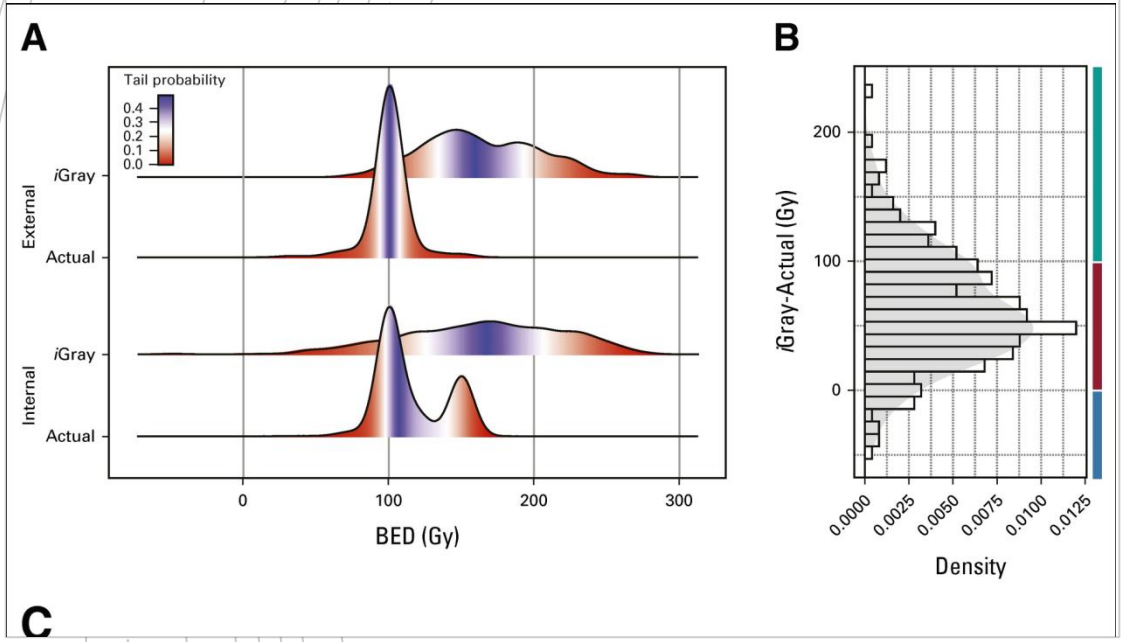

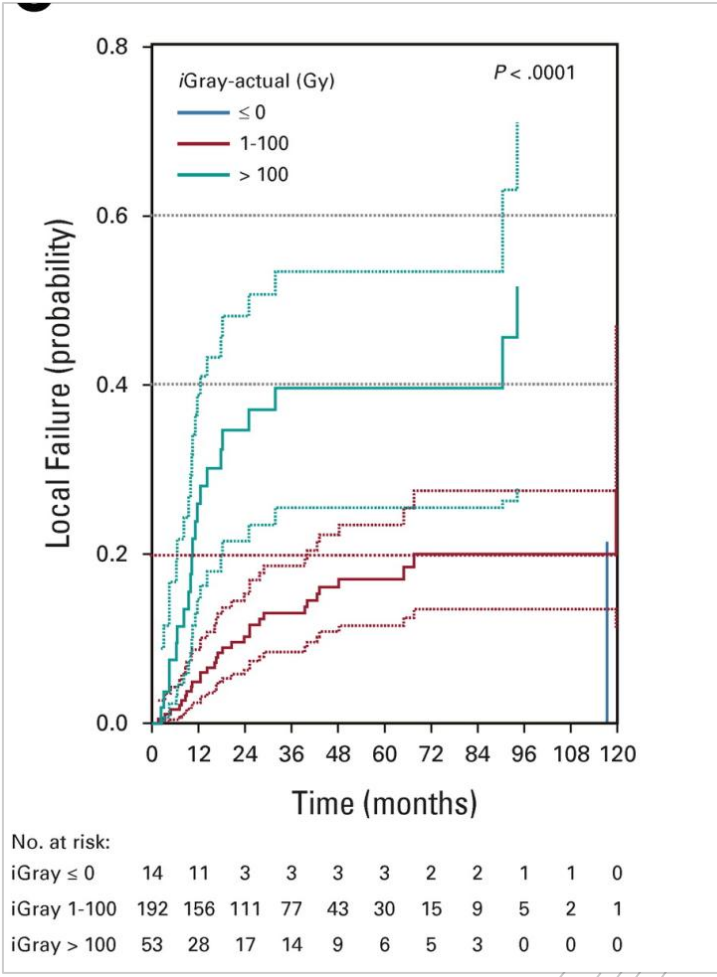

***i*Gray, an individualized radiation dose estimate that projects a treatment failure probability of < 5% at 24 months**

AI guided treatment

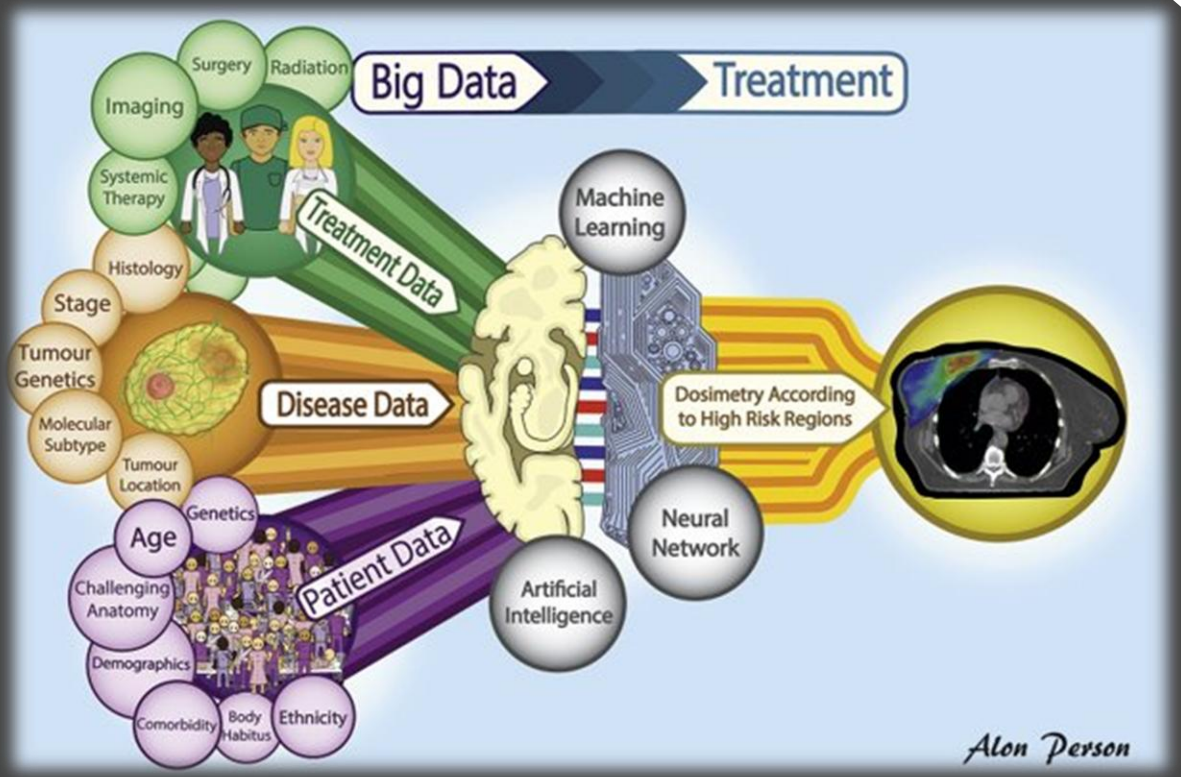

Radiotherapy treatment delivery

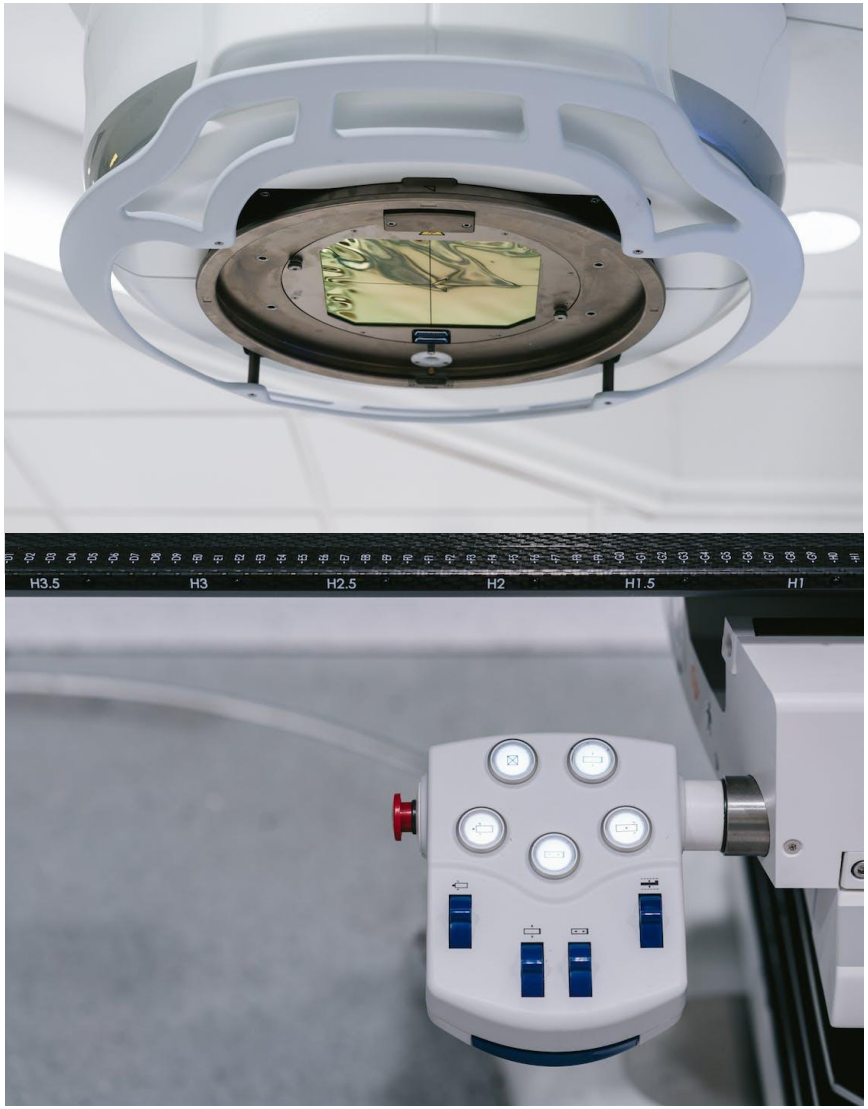

Target localization for IGRT

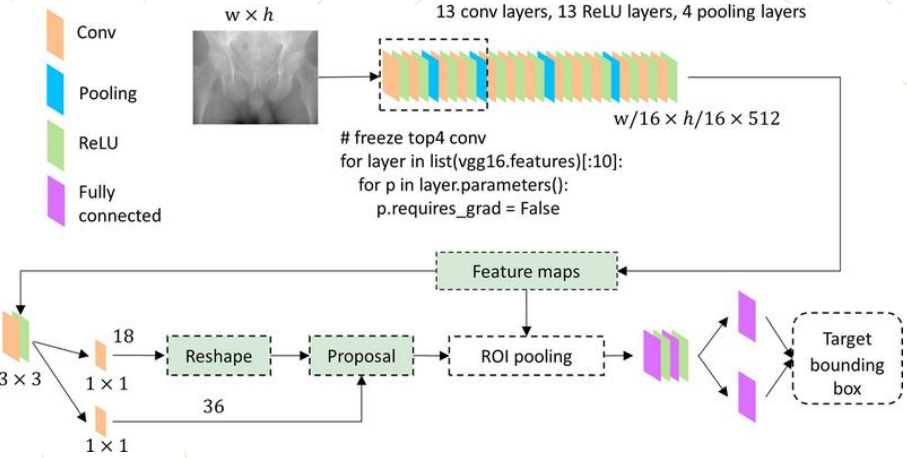

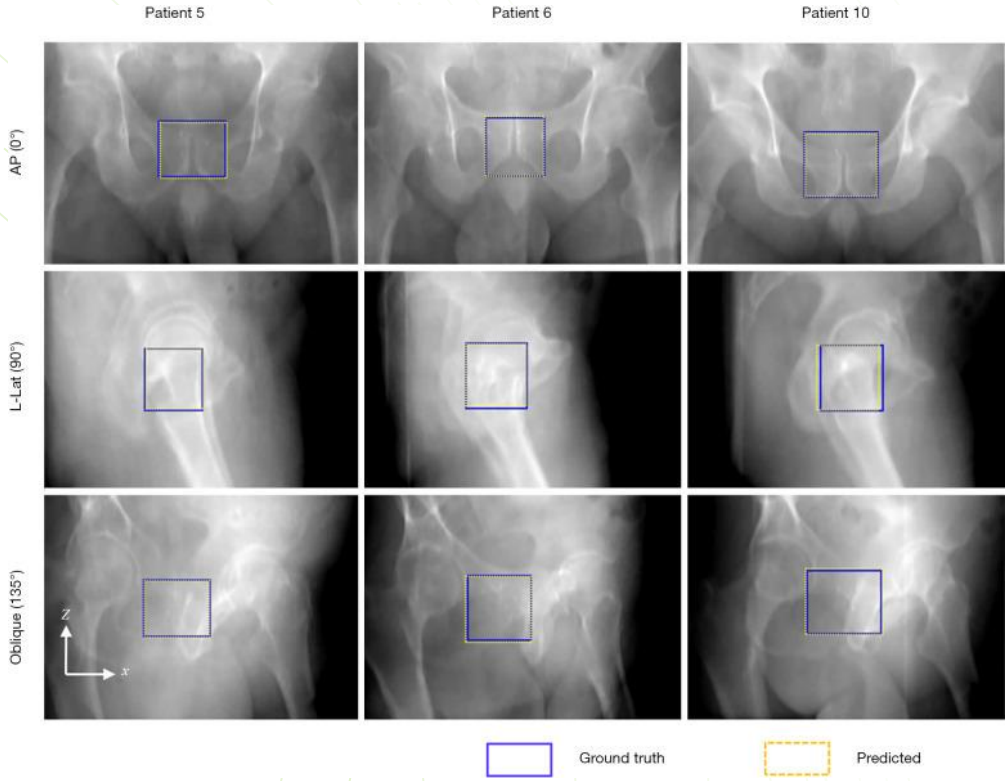

Zhao, Radiotherapy and Oncology, 2020

Deformable image registration

- GAN

dAUTOMAP: fast image reconstruction from undersampled k-space

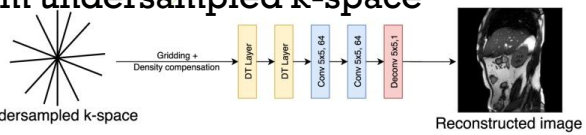

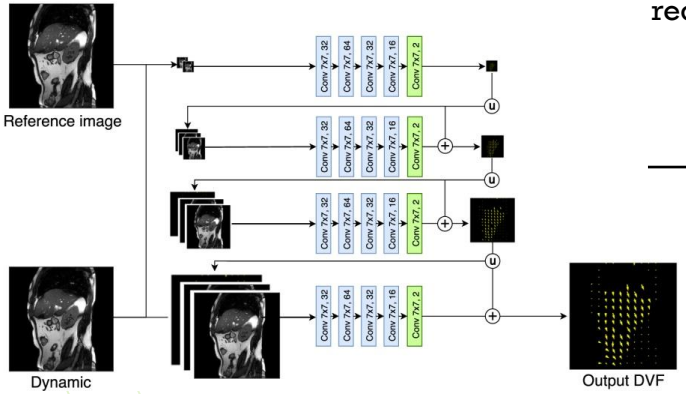

Spynet: CNN motion estimation

Time (acquisition/ reconstruction/motion (ms))	
R=10	100/5/15
R=20	50/5/15
R=25	40/5/15

Comparison w traditional methods

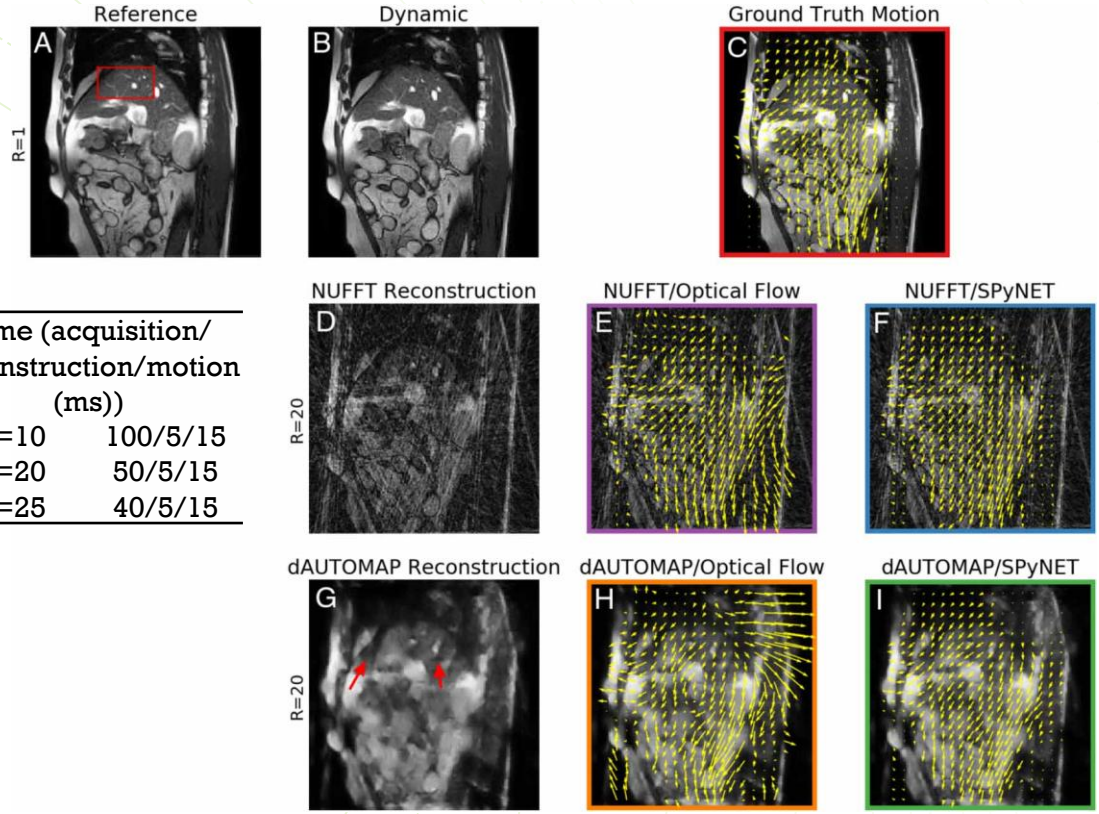

Terpstra et al, Physics in Medicine & Biology, Volume 65, Num

Tumor Tracking by AI

Tumor centroid prediction:

- LSTM (Long Short Term Memory) networks (AI)

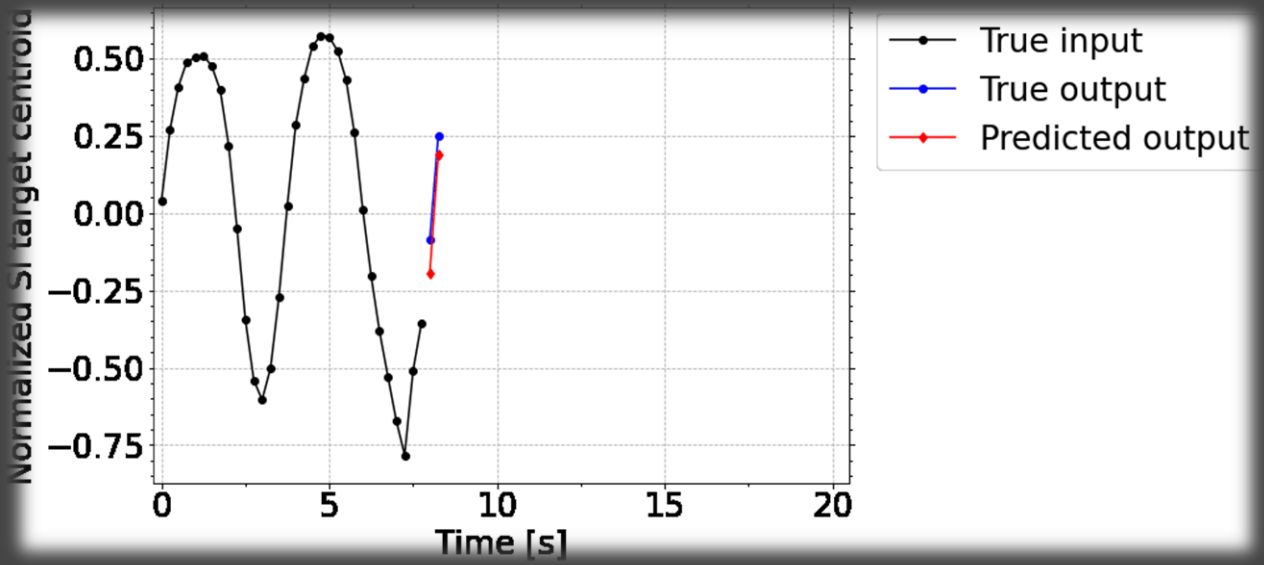

LMU KLINIKUM

Gemelli

Fondazione Policlinico Universitario Agostino Gemelli IRCCS
Università Cattolica del Sacro Cuore

ART
Advanced Radiation Therapy

Courtesy of Marco Riboldi, AAPM 2023, Houston, TX

Patient selection for breath-hold RT

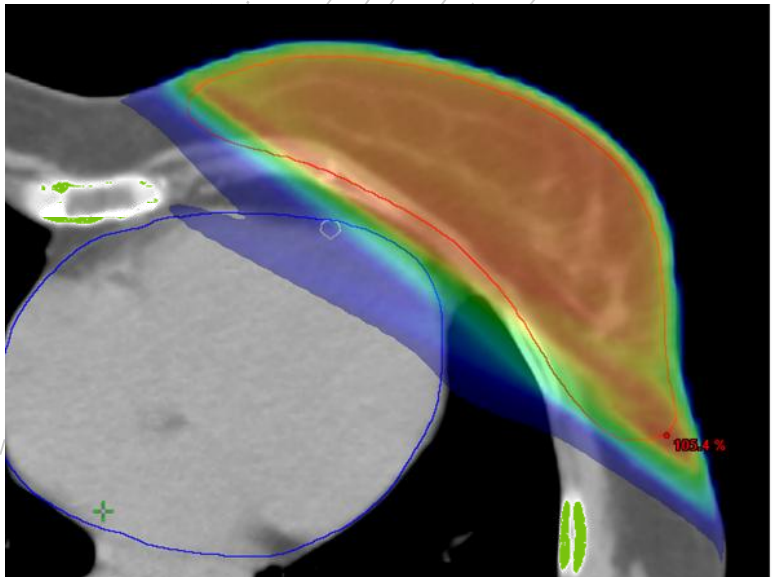

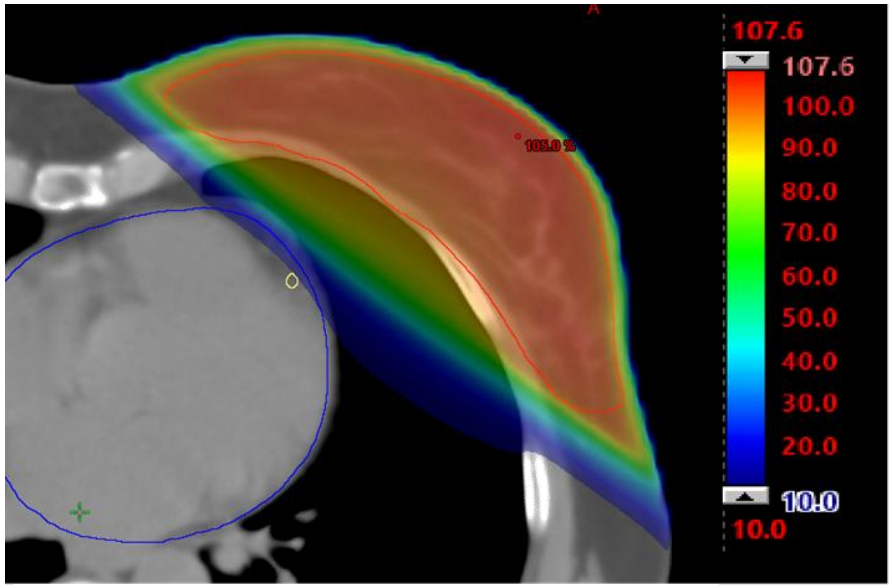

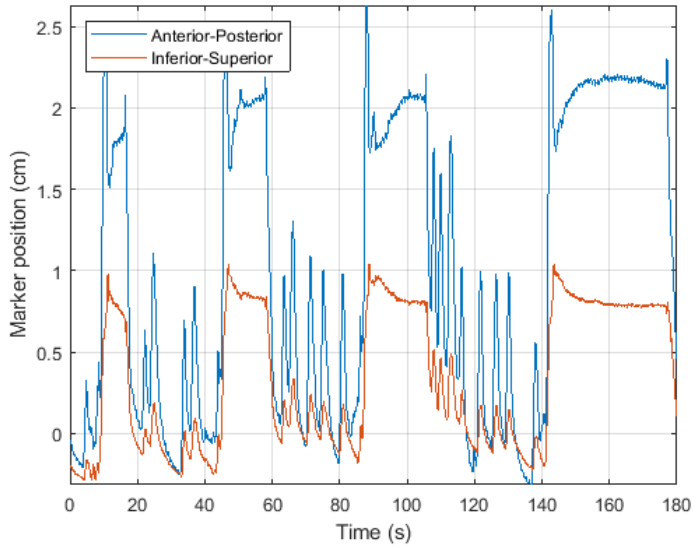

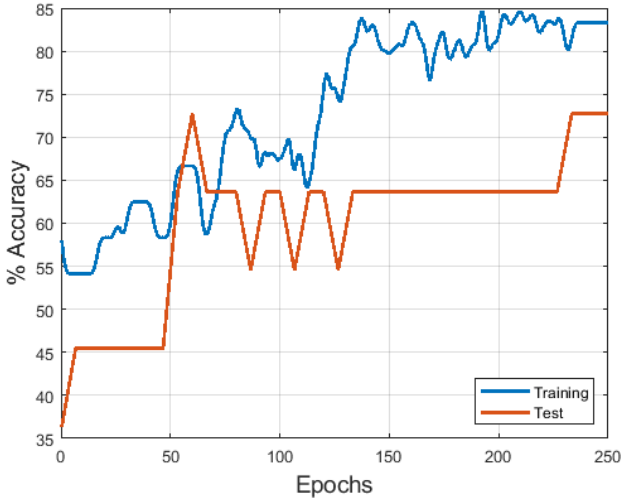

Vendrame, Applied Sciences, 2023

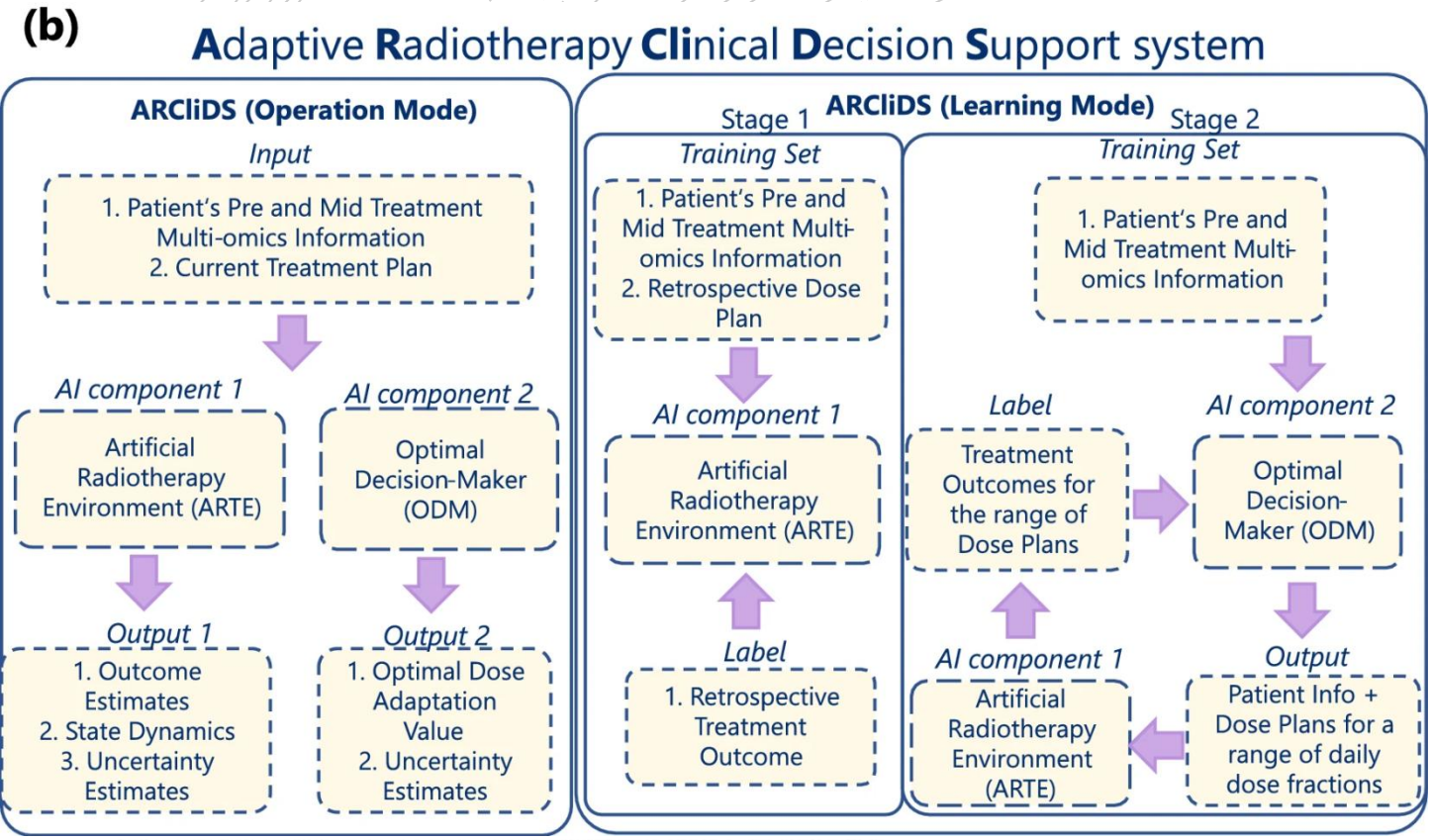

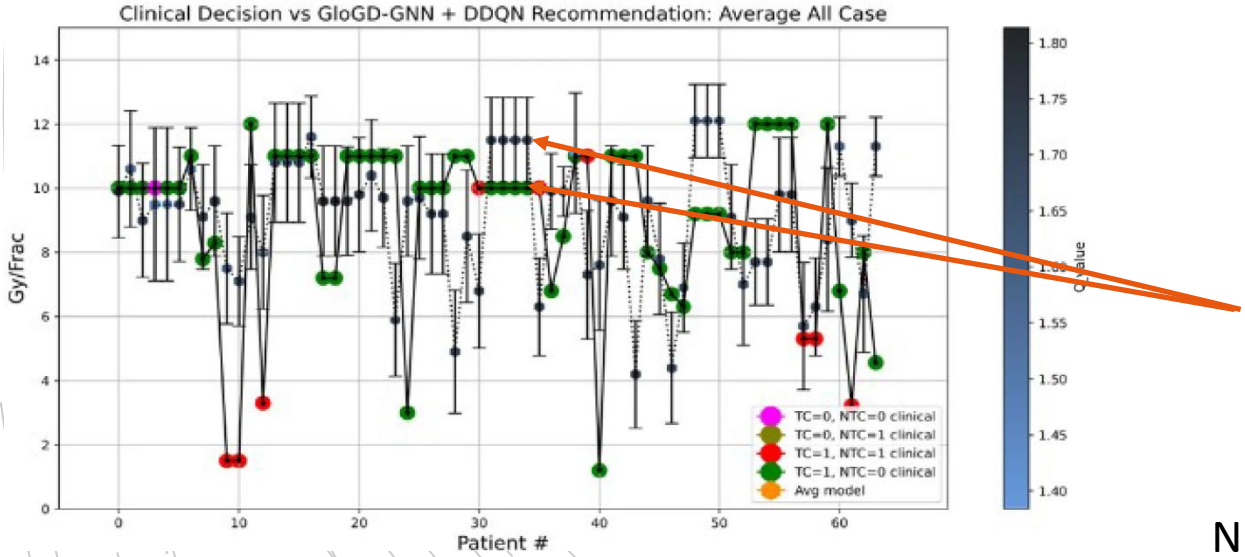

Treatment adaptation

Blue dots = adapted fraction dose by AI
Other colors = adapted by human

Niraula, Scientific Reports, 2023

Radiotherapy follow-up

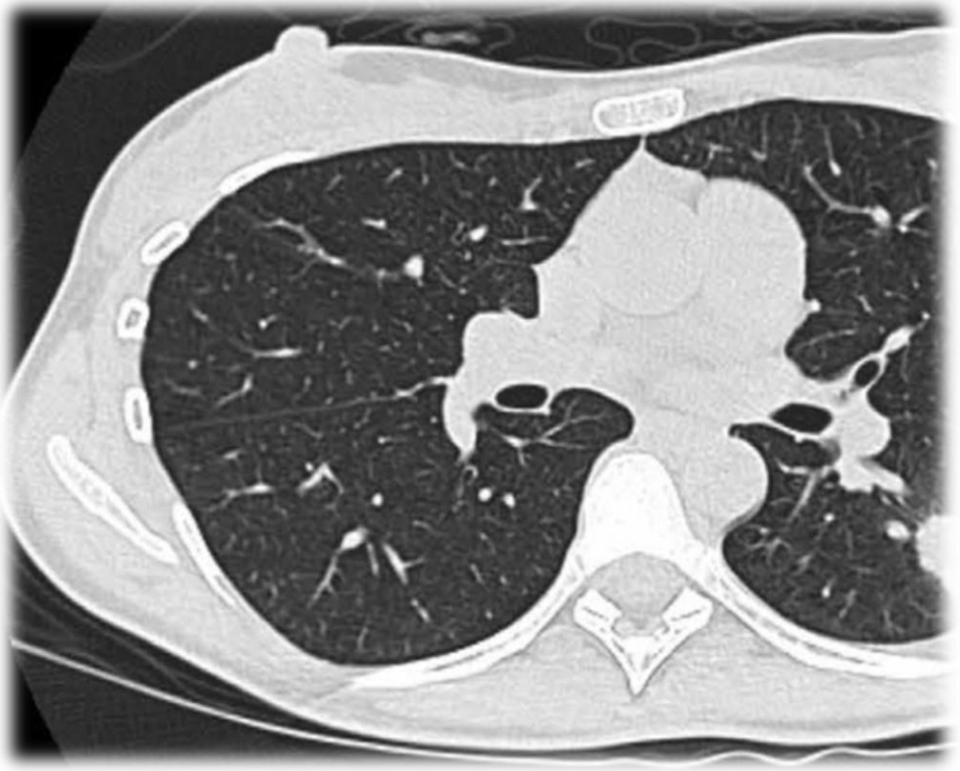

Differentiation of relapse from fibrosis

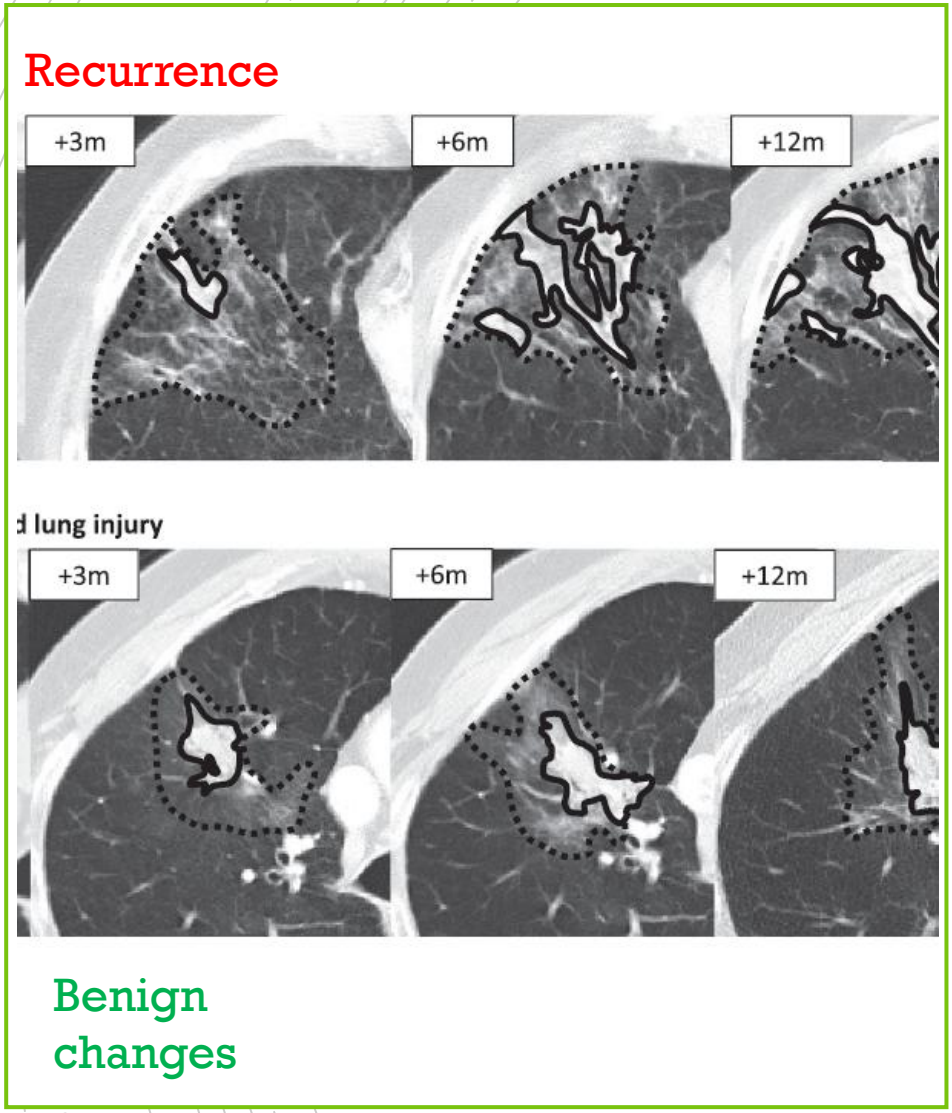

- Accuracy 76%–77% of radiomic features in cross-validation

Mattonen et al. Med. Phys. 41 (3), March 2014

Radiotherapy QA

Automated QA of treatment plans

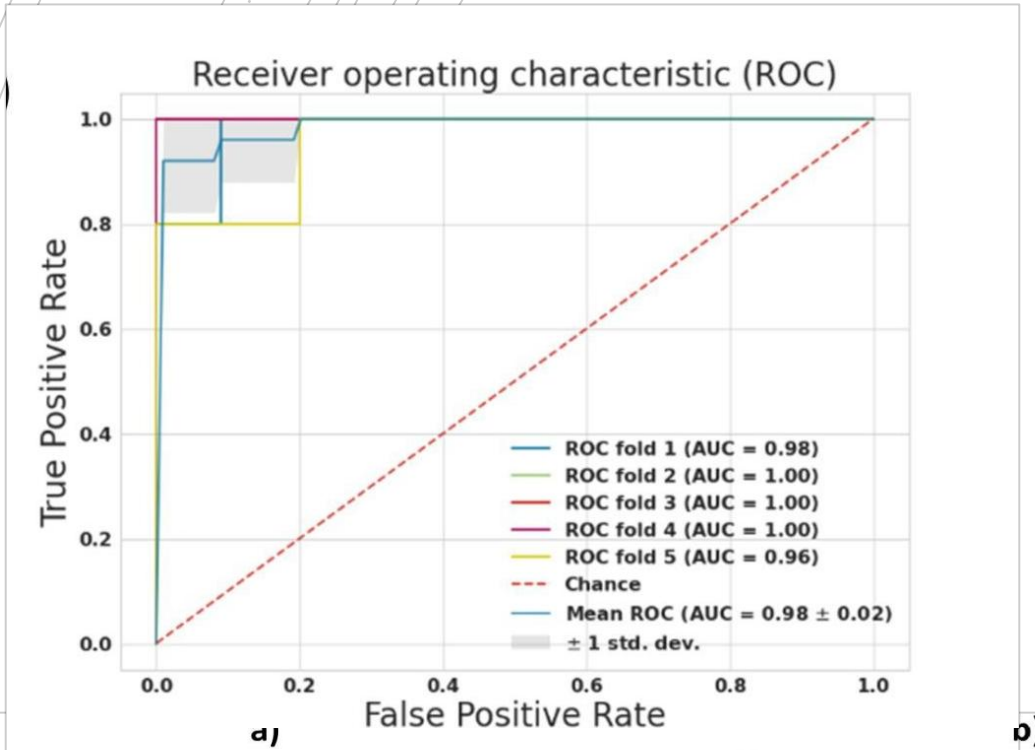

- class-0 plans for which the PTV objective was met
- class-1 plans for which the PTV objective was not met due to the priority trade-off to meet one or more organs-at-risk constraints.

Siciarz,
Clinical and Translational Radiation Oncology
2021

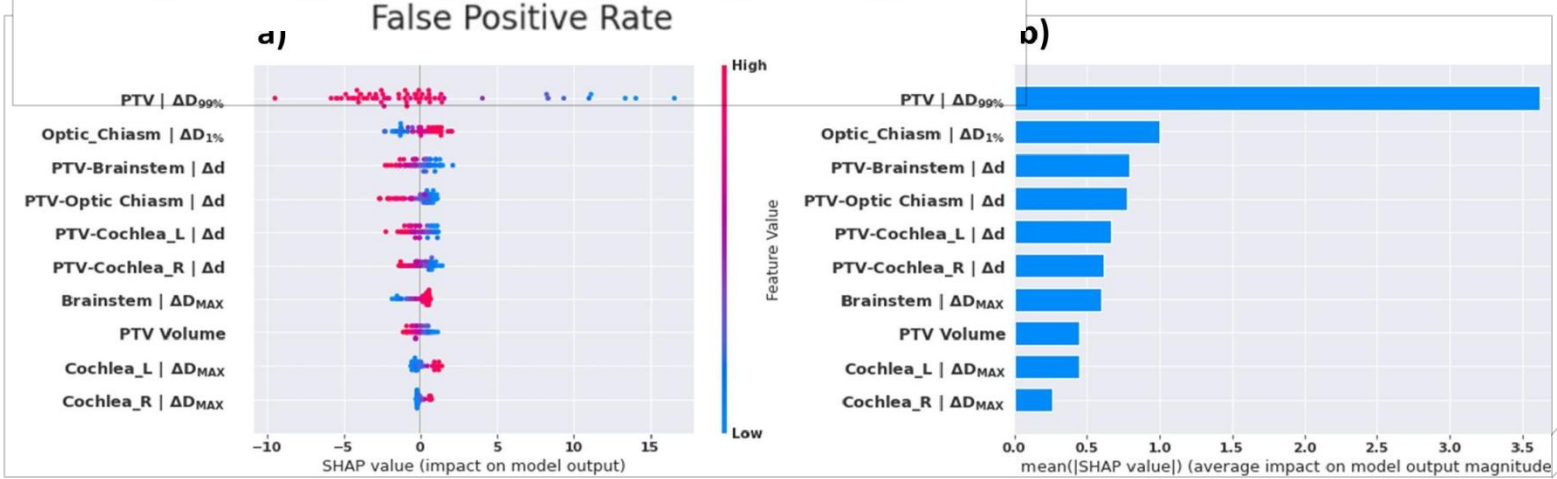

Quality check of treatment plans

Table 1. Example potential error cases.

Tx_Intent (site)	Technique	Modality	Dose_Ttl	Dose_Tx	numFields	Severity
Palliative (Brain)	Conformal Plan	×06	**5400**	200	6	7
Curative (Brain)	IMRT	**×18**	6000	200	12	2
Palliative (Breast)	PA	×18	2268	**81**	2	8

Note: Introduced errors are indicated in bold.

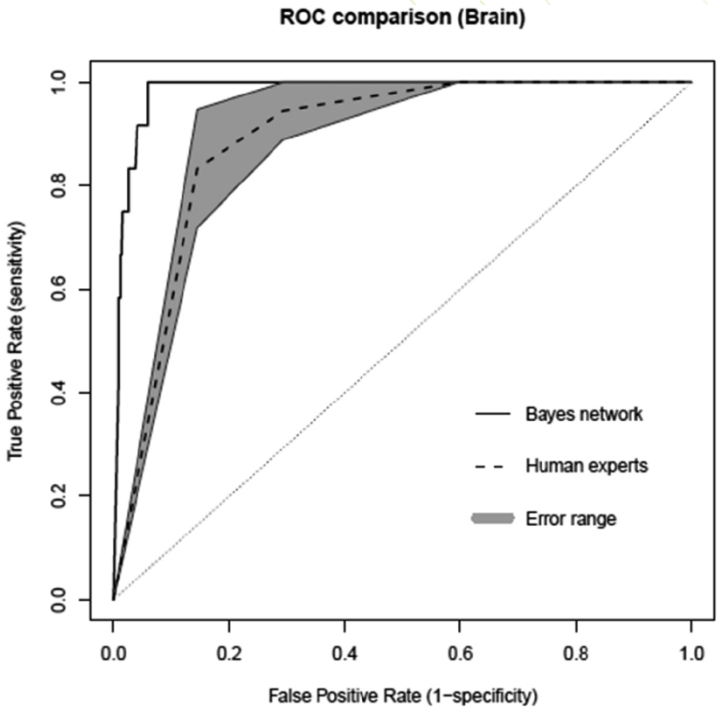

Alan M Kalet 2015 Phys. Med. Biol.

Automated QA of LINACs by AI

- **Prediction of results of Delivery Quality Assurance (DQA) of VMAT**

Prediction of Delivery Quality Assurance of VMAT success/failure by ML

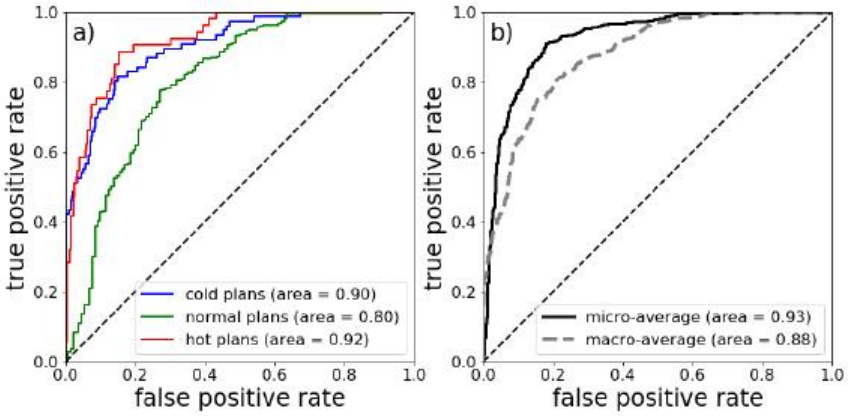

A Granville *et al* 2019 *Phys. Med. Biol.* **64** 095017

prediction of multi-leaf collimator positional errors
Using dynalog files

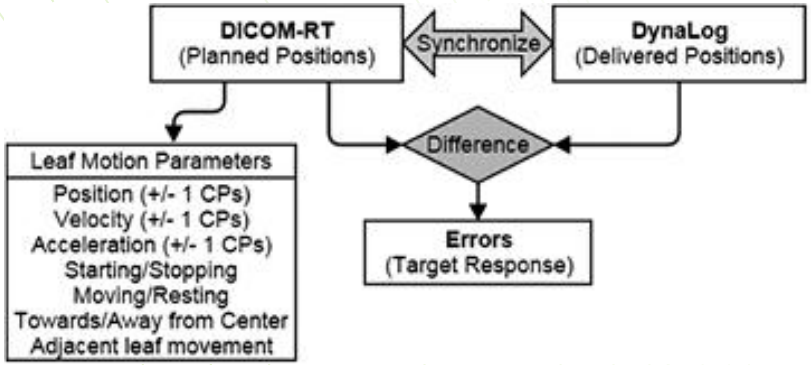

Carlson et al., Phys. Med. Biol. 61:2514.

References	QA Source	Data Source	ML Model	Task
Carlson et al. (2016)	DICOM_RT, Dynalog files	74 VMAT plans	Regression, Random Forest, Cubist	MLC Position Errors Detection
Li and Chan (2017)	Daily QA Device	5-year Daily QA Data	ANN Time-Series, ARIMA Models	Symmetry Prediction
Sun et al. (2018)	Ion Chamber	1,754 Proton Fields	Random Forrest, XGBoost, Cubist	Output for Compact Proton Machine
El Naqa et al. (2019)	EPID	119 Images from 8 Linacs	Support Vector Data Description, Clustering	Gantry Sag, Radiation Field Shift, MLC Offset
Grewal et al. (2020)	Ion Chamber	4,231 Proton Fields	Gaussian Processes, Shallow NN	Output and Patient QA Proton Machine
Osman et al. (2020)	log files	400 machine delivery log files	ANN	MLC Discrepancies during Delivery & Feedback
Chuang et al. (in press)	Trajectory log files	116 IMRT plans, 125 VMAT plans	Boosted Tree Outperformed LR	MLC Discrepancies during Delivery & Feedback
Zhao et al. (in press)	Water Tank Measurement	43 Truebeam PDD, Profiles	Multivariate Regression (Ridge)	Modeling of Beam Data Linac Commissioni

QA of radiotherapy

https://www.frontiersin.org/articles/10.3389/frai.2020.577620/full

Prediction of gamma passing of IMRT plans

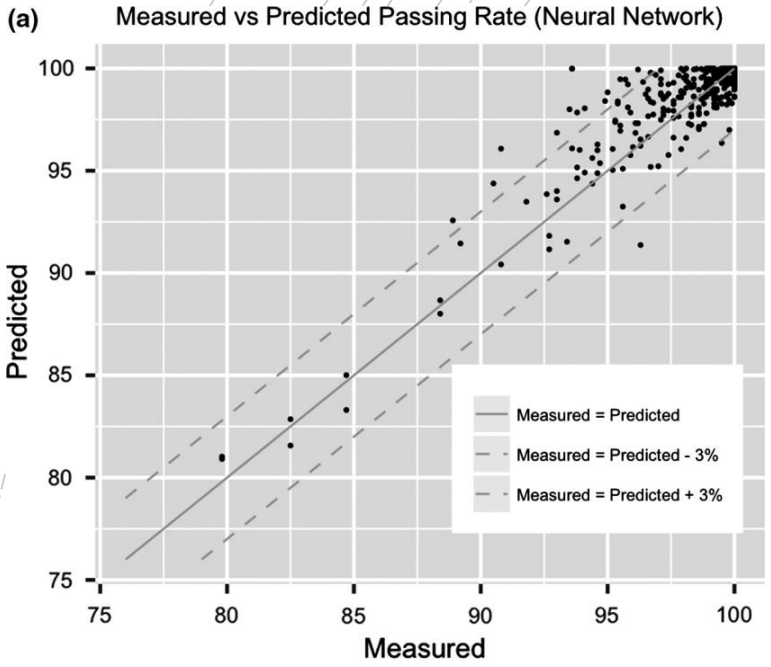

- Dosimetry quality assurance:

Prediction of 3% 3mm gamma passing of IMRT plans rate by CNN

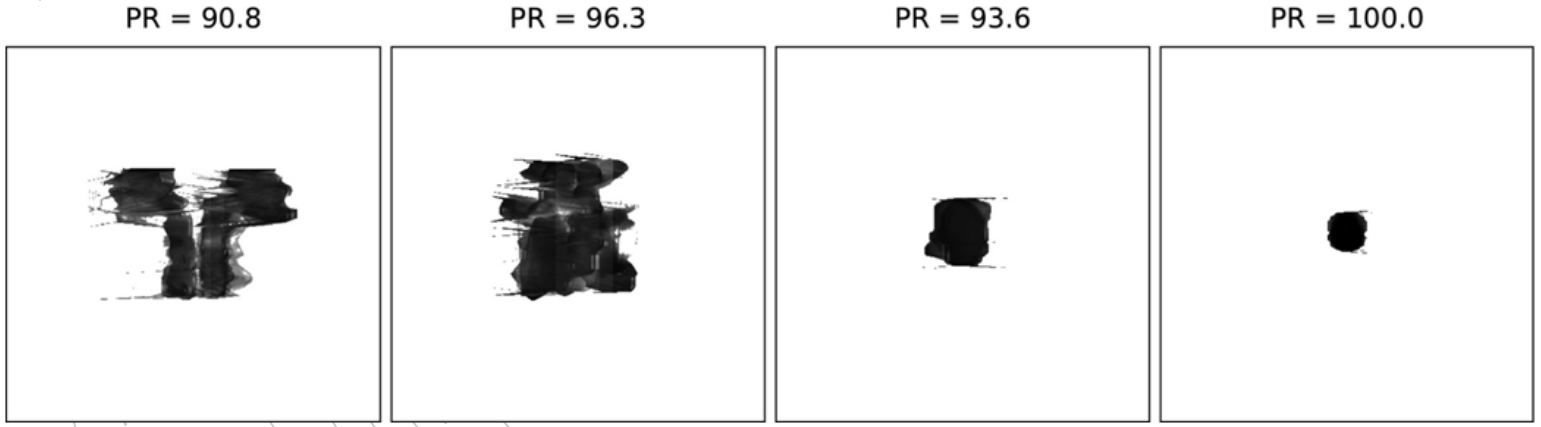

Interian Medical Physics, 2018

Prediction of errors in treatment delivery

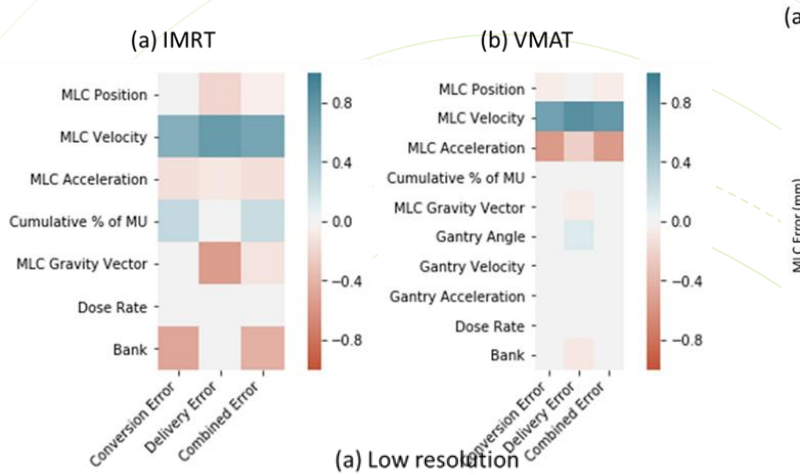

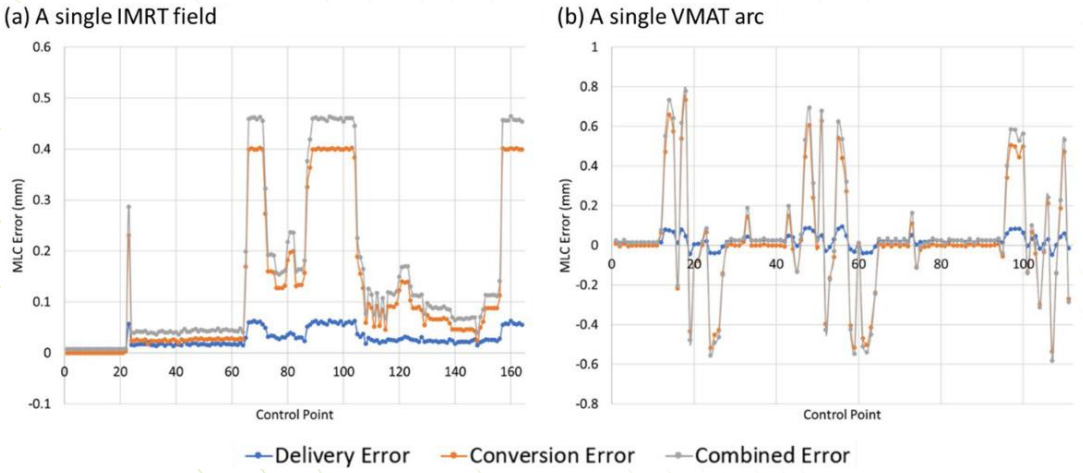

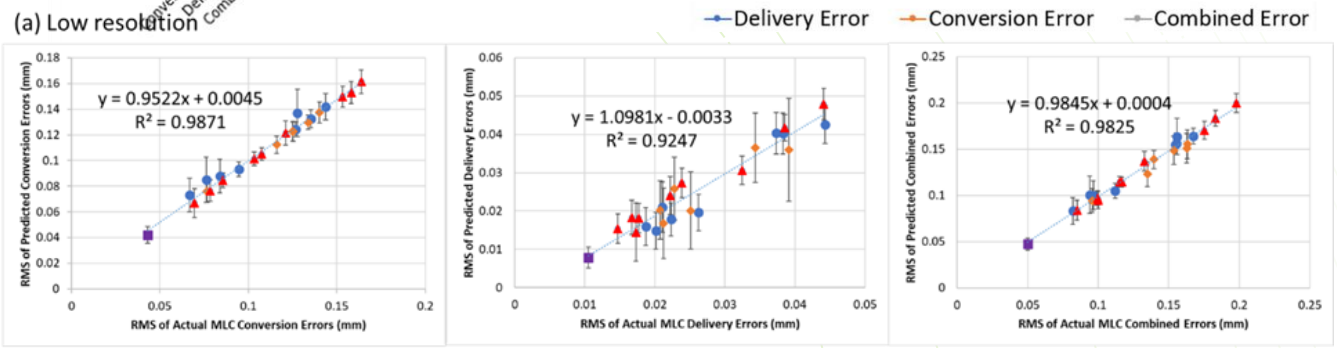

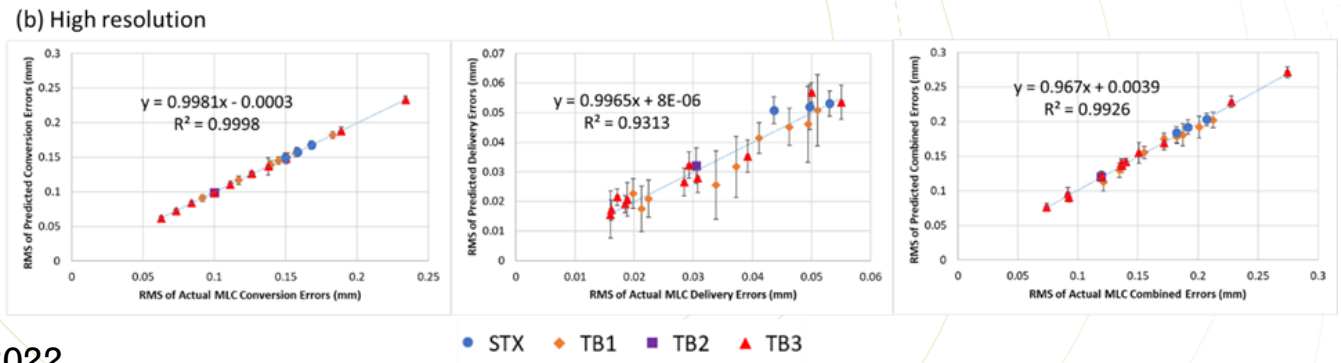

Lay, SoftwareX, 2022

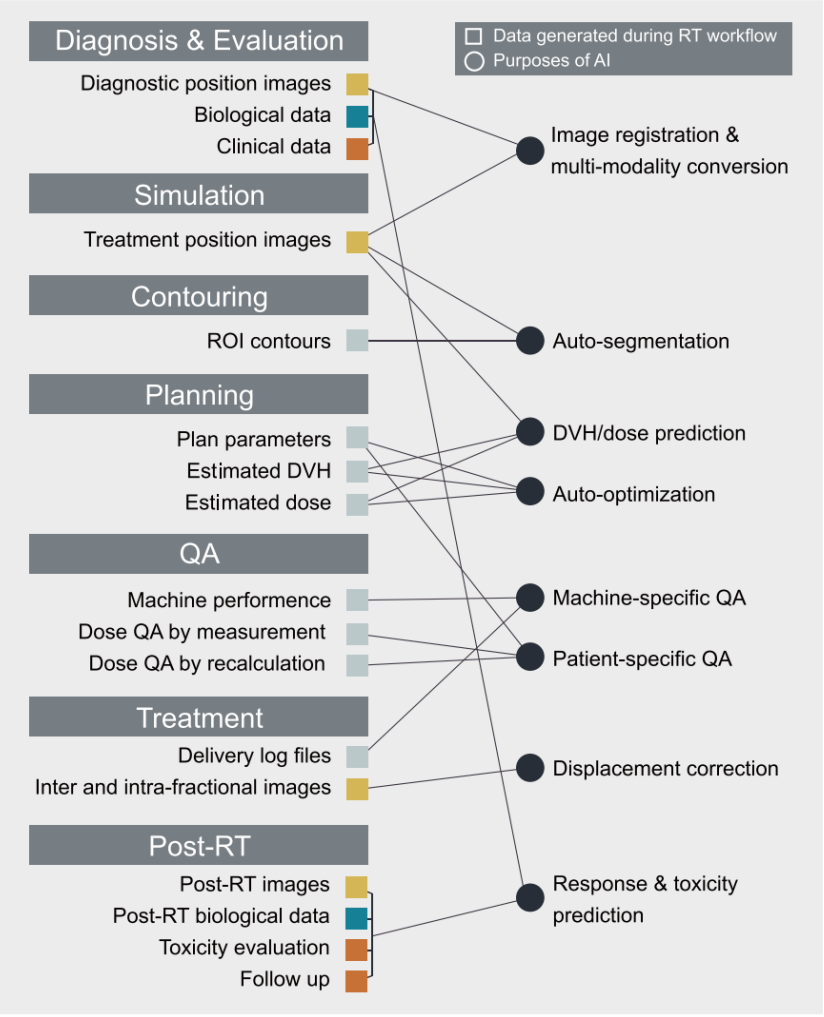

Summary

- Li, Seminars in Cancer Biology 2022

Selected bibliography

Introduction to AI:

- Shen, C.; Nguyen, D.; Zhou, Z.; Jiang, S.B.; Dong, B.; Jia, X. An Introduction to Deep Learning in Medical Physics: Advantages, Potential, and Challenges. *Phys.Med.Biol.* **2020**, *65*, 05TR01-6560/ab6f51, doi:10.1088/1361-6560/ab6f51.

Role of the Medical Physicist:

- 2. Avanzo, M.; Trianni, A.; Botta, F.; Talamonti, C.; Stasi, M.; Iori, M. Artificial Intelligence and the Medical Physicist: Welcome to the Machine. *Applied Sciences* **2021**, *11*, 1691, doi:10.3390/app11041691.

Applications of AI to RT:

- 3. Appelt, A.L.; Elhaminia, B.; Gooya, A.; Gilbert, A.; Nix, M. Deep Learning for Radiotherapy Outcome Prediction Using Dose Data - A Review. *Clin Oncol (R Coll Radiol)* **2022**, *34*, e87–e96, doi:10.1016/j.clon.2021.12.002.
- 4. Vandewinckele, L.; Claessens, M.; Dinkla, A.; Brouwer, C.; Crijns, W.; Verellen, D.; van Elmpt, W. Overview of Artificial Intelligence-Based Applications in Radiotherapy: Recommendations for Implementation and Quality Assurance. *Radiother Oncol* **2020**, *153*, 55–66, doi:10.1016/j.radonc.2020.09.008.